Reconstruction from Non-uniform Samples

by

Kwang Siong Jeremy Leow

B.Eng., Imperial College of Science, Technology and Medicine (2008)

Submitted to the Department of Electrical Engineering and Computer Science
in partial fulfillment of the requirements for the degree of

Master of Science in Electrical Engineering and Computer Science

at the

MASSACHUSETTS INSTITUTE OF TECHNOLOGY

February 2010

Author .....
Department of Electrical Engineering and Computer Science
January 15, 2010

Certified by .....
Alan V. Oppenheim
Ford Professor of Engineering
Thesis Supervisor

Accepted by .....
Terry P. Orlando
Chairman, Department Committee on Graduate Theses

Reconstruction from Non-uniform Samples

by

Kwang Siong Jeremy Leow

Submitted to the Department of Electrical Engineering and Computer Science
on January 15, 2010, in partial fulfillment of the
requirements for the degree of
Master of Science in Electrical Engineering and Computer Science

Abstract

Exact reconstruction of a band-limited signal from its non-uniform samples involves the use of Lagrange interpolation, which is impractical to implement as it is computationally difficult. This thesis develops approximate reconstruction methods based on time-warping to obtain reconstruction of band-limited signals from non-uniform samples. A review of non-uniform sampling theorems is presented followed by an alternative interpretation of the Lagrange interpolation kernel by decomposing the kernel into its constituent components. A discussion of time-warping and its use in the context of non-uniform sampling is made. This includes an alternative interpretation known as the delay-modulation, which we show to be a simpler representation for a specific case of non-uniform sampling where the sample instants are deviations from a uniform grid. Based on some essential characteristics of the Lagrange kernel, a framework using a modulated time-warped sine function is formed to obtain various approximations to the Lagrange kernel. The thesis also formulates a vector space representation of non-uniform sampling and interpolation and incorporates warped sinc functions to obtain faster convergence in iterative algorithms for reconstruction of band-limited signals from non-uniform samples.

Thesis Supervisor: Alan V. Oppenheim
Title: Ford Professor of Engineering

Acknowledgments

As I approach the end of another phase in life, this thesis gives me the opportunity of acknowledging some of the special people who have influenced my life in one way or another.

Professor Oppenheim, otherwise known as Al, has been a great teacher and someone whom I believe to have significantly shaped my thinking, expression and perspective in life. It has been a great journey in learning and I would like to thank you for the support which you have given me throughout my stay at DSPG.

I would also like to thank the past and present members of DSPG including Tom Baran, Petros Boufounos, Sourav Dey, Dan Dudgeon, Zahi Karam, Jon Paul Kitchens, Joseph McMichael, Shay Maymon, Charles Rohrs, Melanie Rudoy, Andrew Russell and Dennis Wei. The weekly group meetings and ad hoc individual discussions were always so creative and interesting. Many of the insights in this thesis were derived from the interaction with these wonderful people. Special thanks goes to Eric for keeping the group running efficiently and for ensuring that we were kept well nourished during our group meetings. I wish everyone in the group well and hope that DSPG will continue to be so interactive and intellectually stimulating.

Social life throughout these 17 months have been much more enjoyable, thanks to my jovial friends in the Singapore community at MIT. I would also like to thank Jonathan and Wenxian for the academic discussions beyond the scope of my research.

Ninghan has been such a great companion, friend, housemate and source of motivation during my time at MIT. I wish her well for her long journey through Ph.D. and I will miss her too.

Most importantly, I would like to show my appreciation and love for my family. Despite my absence from home these past four years, they have always shown their support and concern for me. I am deeply grateful to everyone at home for where I am today.

I believe that education is a lifelong process and my stay at MIT and DSPG has reinforced my joy of learning.

Contents

List of Figures

Chapter 1

Introduction

Reconstruction of signals from their sample values is an important topic in signal processing. Uniform sampling is the most commonly known form of sampling and it occurs when samples or values of continuous-time signals are obtained at equally spaced time intervals. Under certain conditions, a continuous-time signal is recoverable from this set of samples. Though reconstruction from uniform samples is convenient to implement, its limitation lies in the need for the samples to be on a uniform grid.

A more general sampling scheme involves the notion of non-uniform sampling, which is an extension of uniform sampling without constraining the sample instants to be on a uniform grid. However, reconstruction from non-uniform samples is difficult as absence of a uniform grid structure limits the use of time-invariant processes for reconstructing continuous-time signals. In general, it is difficult to perfectly recover signals from samples taken at an arbitrary set of time instants. Existing reconstruction methods for non-uniform sampling assume some form of structure inherent in the sampling process that can be used for recovering continuous-time signals.

Non-uniform sampling arises naturally in many data acquisition problems and can be implemented in a rich variety of applications. Such applications typically require a high degree of accuracy in the reconstruction process. For instance, an important application of reconstructing signals from jittered samples occurs in biomedical devices. These devices can be low-power energy scavenging sensors that use self-timed circuits, thus removing the need for clock buffers and clock distribution that require large power consumption. However, these self-timed circuits tend to introduce jitter in the sampling processor of the signal

processing chip [1]. In biomedical applications such as wearable heartbeat detectors, an accurately reconstructed electrocardiogram (ECG) signal from the jittered samples is especially important to prevent false alarms and misses in the detection of cardiac arrhythmia.

Another application of non-uniform sampling is in time-interleaved analog-to-digital converters (TI-ADCs), where a signal is passed through multiple parallel channels, each uniformly sampling the signal at the same rate. The output samples of the channels are then multiplexed to obtain a full discrete-time representation of the signal. In the case where the clock phases of these channels are asynchronous, interleaving samples from each channel leads to recurrent non-uniform sampling. Recurrent non-uniform sampling can also be found in sensor networks. Each sensor uniformly samples the environment asynchronously and transmits a signal to a base station. The resultant signal obtained at the base station takes the form of recurrent non-uniform sampling.

In addition to time domain processes, non-uniform sampling can also arise in either the spatial or frequency domains. Such examples can be found in the non-uniform spacing of elements in antenna arrays, and in towed acoustic arrays for underwater measurement, to trade off between the length of the array and the number of elements. Non-uniformity of the array element spacing is sometimes part of the array design, where for example, these arrays have logarithmically spaced intervals. In some other cases, it might be the failure of an array element in uniformly spaced arrays, and this corresponds to sampling with a single missing sample instant from a set of uniform sample points.

Another potential application of non-uniform sampling involves sampling based on time-varying signal parameters. Signals which can be characterized by a set of parameters, are usually more efficiently represented if information about these parameters is factored into the sampling instants. One such example as mentioned earlier are signals with fluctuations in their local bandwidths. An efficient representation of such signals can be obtained by sampling them based on their local bandwidths or characteristics, thus leading to a lower overall sampling rate [29].

1.1 Background

One approach to reconstruction of band-limited signals from non-uniform samples is through Lagrange interpolation. The Lagrange interpolation formula originated as an attempt to

find a polynomial function that takes on N function values, f_n associated with N distinct time instants, t_n. For reconstruction from non-uniform samples of band-limited signals, the Lagrange interpolation series can be regarded as having infinitely many constraint points.

In the context of non-harmonic Fourier series, Paley and Wiener [21] studied the relationship between the Lagrange interpolation formula and the complex exponentials $\{e^{j\lambda_n x}\}$ in $L^2(-\pi, \pi)$ by imposing the constraint of $|\lambda_n - n| < \frac{1}{\pi^2}$ where $n \in \mathbb{Z}$. By relating to non-uniform sampling, this corresponds to having the sample instants deviate by a bounded amount from the uniform grid. Levinson [18] then showed that the best possible bound is $|\lambda_n - n| < \frac{1}{4}$ and given this constraint, Kadec [15] showed that the set $\{e^{j\lambda_n x}\}$ forms a Riesz basis in $L^2(-\pi, \pi)$.

In his seminal paper on non-uniform sampling of band-limited signals [33], Yen introduced several reconstruction theorems, mainly to deal with a finite number of non-uniform samples on an otherwise uniform grid, the missing sample problem and recurrent non-uniform sampling. These reconstruction theorems were shown without reference to Lagrange interpolation. It was later in the work of Yao and Thomas [32] that the Lagrange interpolation functions were applied to reconstruct band-limited signals from non-uniform samples. Separately, Higgins introduced non-uniform sampling theorems for band-limited functions using an approach based on reproducing kernel Hilbert spaces [14].

Application of time-warping methods were used by Papoulis in [22] as a means to reconstruct band-limited signals from jittered samples. In [5] and [36], time-warping was used for reconstruction from samples of functions in the space of locally band-limited signals.

One practical approach to recovering a signal from its non-uniform samples is the use of non-uniform splines. Iterative reconstruction methods for non-uniform sampling are discussed in [9] - [11]. Some of the other discussions of non-uniform sampling revolve around reconstruction of signals from recurrent non-uniform samples. These can be found in [8]. Hardware implementation of non-uniform sampling are discussed in [27]. For a good review of literature concerning other techniques in non-uniform sampling, one can refer to [13] and [19].

1.2 Outline of the Thesis

Exact reconstruction methods to recover band-limited signals from non-uniform samples require knowledge about the non-uniform sampling grid. Subject to certain conditions, reconstruction of a band-limited signal from non-uniform samples can be done through Lagrange interpolation. However, the Lagrange kernel is impractical to implement due to its computational complexity and large dynamic range. The importance of non-uniform sampling of continuous-time signals in real-world applications and the complexity involved in signal reconstruction drive the need for simple reconstruction techniques. This thesis develops some approximate reconstruction methods for reconstruction of one dimensional signals from their non-uniform samples.

Chapter 2 reviews some of the important concepts in non-uniform sampling theory. The notion of sampling density is introduced as an analogue to sampling frequency. Other concepts such as a set of uniqueness, stable sampling and interpolation are also discussed with reference to similar concepts in the uniform sampling case. A general system is formulated for analysis and synthesis of signals, where the composing functions of these kernels can either be bases or frames. Next, we present the non-uniform sampling theorem which states that the Lagrange kernel perfectly reconstructs band-limited signals from non-uniform samples, when the deviations of the sampling instances from a uniform grid are smaller than a certain factor. In the last part of chapter 2, the Lagrange interpolation formula is interpreted as a system in which the kernel is separated into several components. A frequency domain view of this system is presented for uniform sampling as an illustration.

Chapter 3 introduces the idea of time-warping of signals and discusses its applications, advantages and limitations. An interpretation of time-warping referred to as delay modulation is developed, which is suitable for characterizing non-uniform sampling for the case when the sample instants are deviations from a uniform grid. Two different approaches for determining the inverse warped signal are described. Time-warping is then applied to non-uniform sampling by showing the different equivalent sampling systems. Different two-dimensional input-output representations of delay modulation are also obtained and approximations to time-warping functions as well as the Fourier transform of warped signals are made.

Chapter 4 uses the system-level interpretation of the Lagrange kernel to study the

characteristics of the Lagrange interpolation function and its components. Various forms of approximations to the component are made while maintaining their essential characteristics. Approximations include the shifted-sinc function, reconstruction by assuming sampling on the uniform grid, piecewise sinusoidal approximation and non-uniform spline approximation. A numerical experiment is done to show the result of the approximations by comparing them with cubic spline interpolation of the samples.

Chapter 5 builds on an abstract vector space representation of non-uniform to show the relationship between out-of-band frequency components and in-band frequency components. Warped sinc kernels are then formulated as projections, which we use to modify an iterative reconstruction, introduced by Grochenig et. al., to obtain fast convergence rates.

Chapter 2

Construction of Band-limited Signals on a Nonuniform Grid

In this chapter, some of the important concepts of non-uniform sampling theory are introduced. We make a distinction between the analysis and synthesis processes by highlighting the need to consider both sampling and reconstruction time instants. We discuss the density conditions necessary for reconstruction of band-limited functions. A framework for time-dependent signal representation (analysis) and reconstruction (synthesis) is also presented. This framework is used to review some of the sampling theorems presented in [14], [18] and [32]. We conclude by presenting a system interpretation of the Lagrange reconstruction kernel.

2.1 Density of Non-uniform Samples

Sampling theory in general encompasses two stages: sampling and reconstruction. The uniform sampling theorem states that if a function $x(t)$ is band-limited with $X(\omega) = 0$ for $|\omega| > \omega_0$, then $x(t)$ is completely determined by its uniform samples taken at a frequency ω_s, where $\omega_s > 2\omega_0$. The function $x(t)$ can be exactly reconstructed by passing the sample impulse train through an ideal lowpass filter with cutoff frequency ω_r such that $\omega_0 < \omega_r < \omega_s - \omega_0$. The rest of this section deals with band-limited functions, and so we specifically define PW_{ω_0} to be the space of all square-integrable functions, f whose Fourier transform $F(\omega)$ is such that $F(\omega) = 0,\ \forall\ |\omega| > \omega_0$. A more general discussion of sampling theory would encompass the Landau condition which deals with the support of $F(\omega)$ as a union of

a finite number of intervals [16]. However, we leave this as a future work, and this thesis will only focus on the case where $F(\omega)$ is a low-pass signal with its support being a single interval.

A similar distinction between the sampling and reconstruction processes can be made in non-uniform sampling, and the focus of our discussion in this section will be about conditions imposed on the samples and non-uniform sampling grid. In uniform sampling, the sampling rate can be described by one parameter ω_s. The analogue of sampling rate in non-uniform sampling is characterized by the average sampling rate or density of samples. For a set of sampling instances on the real axis $\{t_n\}$, the sampling density is defined as

$$D(t_n) := \lim_{r\to\infty} \frac{\#\{t_n \,:\, t_n \in [-r, r]\}}{2r} \tag{2.1}$$

where # is the cardinality of the set bounded by interval r.

In [17], a distinction is made between a unique reconstruction of $f(t)$ and reconstructing $f(t)$ in a stable way. A set $\{t_n\}$ is a set of uniqueness for $f \in PW_{\omega_0}$ if $f(t_n) = 0,\ \forall\ n \in \mathbb{Z}$ implies that $f(t) = 0$. This means that samples of $f(t)$ taken at a set of uniqueness $\{t_n\}$ determine the function $f(t)$ uniquely. It is also possible for a set of uniqueness to have arbitrarily low density and such an example occurs in parametric signal identification where a finite number of samples is sufficient to perfectly reconstruct the signal.

A set $\{t_n\}$ is referred to as a set of stable sampling for $f \in PW_{\omega_0}$ if

$$\int_{-\infty}^{\infty} |f(t)|^2 dt \leq C \cdot \sum_{n=-\infty}^{\infty} |f(t_n)|^2 \tag{2.2}$$

where C is a constant which is independent of $f(t)$. The condition in Eqn. (2.2) ensures that errors in the reconstruction of $f(t)$ are bounded by errors in the sample values [13]. Furthermore, if $\{t_n\}$ is a set of stable sampling, the sampling density cannot be lower than the Nyquist rate and so $D(t_n)$ satisfies

$$D(t_n) \geq \frac{\omega_0}{\pi}. \tag{2.3a}$$

A set of stable sampling always implies a set of uniqueness. This can be shown using Eqn. (2.2) where the sample values $f(t_n) = 0,\ \forall\ n \in \mathbb{Z}$ ensures that $f(t) = 0$. However, a set of uniqueness does not imply a set of stable sampling since a set of uniqueness can have

an arbitrarily low sampling density while a set of stable sampling has to satisfy the density condition in Eqn. (2.3a).

The time instants $\{t_n\}$ are referred to as a set of interpolation for PW_{ω_0}, if for any set of values $\{a_n\} \in l^2$, there exists a $f \in PW_{\omega_0}$ such that $f(t_n) = a_n,\ \forall\, n \in \mathbb{Z}$. It has been shown in [17] that if $\{t_n\}$ is a set of interpolation, then the sampling density cannot be higher than the Nyquist rate, such that

$$D(t_n) \leq \frac{\omega_0}{\pi}. \tag{2.3b}$$

Therefore, if $\{t_n\}$ does not satisfy Eqn. (2.3b), assigning any square-summable sequence $\{a_n\}$ as values taken at $\{t_n\}$ will not guarantee a function that lies in PW_{ω_0}. Hence, a signal $f \in PW_{\omega_0}$ cannot take any arbitrary values at $\{t_n\}$ that is not a set of interpolation. This means that if a set of values with a corresponding set of time instants over-constrain the moment problem $f(t_n) = a_n$ such that no function band-limited to ω_0 can fulfill the moment problem, then the set of time instants is not a set of interpolation.

From the above definitions, one can easily see that to have a stable reconstruction for f while reconstructing the signal through interpolation, the sampling density has to satisfy

$$D(t_n) = \frac{\omega_0}{\pi}. \tag{2.3c}$$

2.2 Analysis and Synthesis

Sampling and reconstruction of signals can be expressed more generally as signal analysis and synthesis. In the following discussion, we show that in general, the analysis and synthesis kernels are dependent on different sets of time instants. Assume that the signal of interest is a member of a Hilbert space H. Consider two sets of functions $\{s_n(t)\}$ and $\{l_n(t)\}$, both of which span the space H, sampling and reconstructing the signal can be interpreted as a system composed of analysis and synthesis functions. This is expressed as

$$\hat{x}(t) = \sum_{n=-\infty}^{\infty} \langle x(t), s_n(t) \rangle\, l_n(t), \tag{2.4}$$

where $\{s_n(t)\}$ are the analysis functions and $\{l_n(t)\}$ are the synthesis functions. Equivalently by duality, the roles of $\{s_n(t)\}$ and $\{l_n(t)\}$ can be interchanged such that $\{l_n(t)\}$ is the set

of analysis functions and $\{s_n(t)\}$ is the set of synthesis functions.

A block diagram representation of Eqn. (2.4) is shown in Fig. 2-1. The inner product of $x(t)$ with the set of analysis functions $\{s_n(t)\}$ is represented by filtering $x(t)$ with a set of time-dependent filter banks $\{s_n(t_n - t\,;\, t_n)\}$, followed by sampling each channel at time instants, t_n. The impulse $a_n\delta(t - t_n)$ is passed through an impulse-to-sample converter (I/S) to obtain the discrete-time samples a_n. These samples, a_n, are then passed through a sample-to-impulse converter (S/I) which creates an impulse at time instant τ_n. The impulse $a_n\delta(t - \tau_n)$ is thereafter filtered with $l_n(t + \tau_n\,;\, \tau_n)$. From Fig. 2-1, the composing function $l_n(t)$ is represented by the sample-to-impulse converter and the synthesis filter $l_n(t+\tau_n\,;\, \tau_n)$. The dependence of synthesis filters on another set of time instants $\{\tau_n\}$ indicates that the synthesis filters do not necessarily have to depend on the sampling instants $\{t_n\}$. The dual system can be described in a similar manner with $\{s_n(t)\}$ and $\{l_n(t)\}$ interchanged.

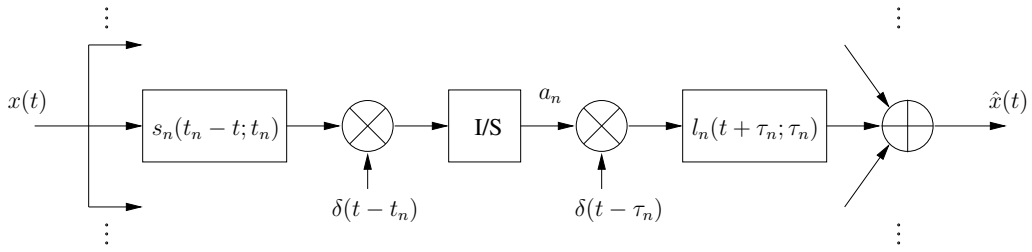

Figure 2-1: Analysis and synthesis systems

The analysis and synthesis functions can either be bases or frames. No restriction on either type has been placed in the formulation. The sets of functions, $\{s_n(t)\}$ and $\{l_n(t)\}$, are bases when the sampling density is as given in Eqn. (2.3c). For the case of oversampling, the sets of functions over-represent the PW_{ω_0} space and correspond to frames. The set of functions $\{s_n(t)\}$ is called a frame if, for every $x \in PW_{\omega_0}$,

$$A\,\|x(t)\|^2 \leq \sum_n |\langle x(t), s_n(t)\rangle|^2 \leq B\,\|x(t)\|^2 \tag{2.5}$$

where A and B are called the frame bounds.

For the special case of uniform sampling at the critical sampling rate of $2\omega_0$, the analysis and synthesis functions are both sinc functions and are orthonormal bases for PW_{ω_0}. However, for non-uniform sampling, the analysis and synthesis functions are not necessarily

equal. The following analyses are described by Higgins [13]. If either the set of analysis or synthesis functions is a Riesz basis for PW_{ω_0}, then its biorthonormal basis, or dual basis is also a Riesz basis. Since both $\{s_n(t)\}$ and $\{l_n(t)\}$ are Riesz bases, then

$$A \sum_n |\langle x(t), s_n(t)\rangle|^2 \leq \left\| \sum_n \langle x(t), s_n(t)\rangle \, l_n(t) \right\|^2 \leq B \sum_n |\langle x(t), s_n(t)\rangle|^2 \tag{2.6}$$

where A and B are positive constants. The left inequality of Eqn. (2.6) implies the convergence of the square-summable sequence $\{a_n\}$ where

$$a_n = \langle x(t), s_n(t)\rangle \,, \tag{2.7}$$

while the right inequality shows the stable sampling property. In addition, $\{s_n(t)\}$ being a Riesz basis also implies that $\{t_n\}$ is a set of interpolation. Therefore from Eqns. (2.3), this means that if $\{s_n(t)\}$ or $\{l_n(t)\}$ is a Riesz basis for PW_{ω_0}, then the sampling density must be equal to $\frac{\omega_0}{\pi}$.

If $\{s_n(t)\}$ is a frame for PW_{ω_0}, then

$$A \|x(t)\|^2 \leq \sum_n |\langle x(t), s_n(t)\rangle|^2 \leq B \|x(t)\|^2 \tag{2.8}$$

where A and B are positive constants. The left inequality of Eqn. (2.8) shows the stable sampling property, while the right inequality shows the convergence of the square-summable sequence $\{t_n\}$. This implies that the sampling density satisfies Eqn. (2.3a), which indicates oversampling.

In practical analysis and synthesis of signals, it is sometimes difficult to establish the dual of a set of functions and so approximations to the duals are usually made. Generalizing the system shown in Fig. 2-1 allows for freedom in designing the analysis and synthesis functions while satisfying certain constraints.

2.3 Reconstruction of Band-limited Signals Using Lagrange Interpolation

Perfect reconstruction of band-limited signals from non-uniform samples uses the Lagrange interpolation formula subject to constraints imposed on the sample instants. In this section,

the series expansion of a band-limited function based on its non-uniform samples will be discussed, and the properties related to Lagrange reconstruction will be elaborated upon.

The non-uniform sampling theorem in [32] states that a signal $x(t)$, belonging to the class of functions band-limited to $\omega_0 = \frac{\pi}{T}$ rad/s, can be represented as a series expansion given by

$$x(t) = \sum_{n=-\infty}^{\infty} x(t_n) l_n(t) \,, \tag{2.9}$$

if the sequence of sampling instants, $\{t_n\}$ is constrained by

$$|t_n - nT| < \frac{T}{4}, \quad \forall\, n \in \mathbb{Z} \,, \tag{2.10}$$

where T is the sampling period. The set of composing functions $\{l_n(t)\}$ is unique and is comprised of Lagrange interpolation functions which belong to PW_{ω_0} [34], and are given by

$$l_n(t) = \frac{G(t)}{G'(t_n)(t - t_n)} \tag{2.11a}$$

where

$$G(t) = (t - t_0) \prod_{k=-\infty}^{\infty} \left(1 - \frac{t}{t_k}\right) \left(1 - \frac{t}{t_{-k}}\right). \tag{2.11b}$$

The following discussion examines the properties of the Lagrange reconstruction formula described in Eqns. (2.9) - (2.11). It is shown in [32] that the composing functions $\{l_n(t)\}$ belong to PW_{ω_0}. Higgins [13] states, with reference to a theorem by Kadec, that if the constraint on the sample instants as given in Eqn. (2.10) is satisfied, then the set $\{e^{j\omega t_n}\}$ forms a Riesz basis for the Hilbert space $L^2[-\frac{\pi}{T}, \frac{\pi}{T}]$. Since $\{e^{j\omega t_n}\}$ is a Riesz basis, there also exists a unique sequence, $\{\varphi_n(\omega)\}$ which by duality is also a Riesz basis.

Using the interpolation property, where

$$l_n(t_k) = \begin{cases} 1, & n = k \\ 0, & n \neq k \end{cases} \,, \tag{2.12}$$

the set of Lagrange interpolation functions, $\{l_n(t)\}$ can be shown to be biorthonormal to the set of shifted sinc functions. If $\{l_n(t)\}$ is the inverse Fourier transform of the set of dual

basis $\{\varphi_n(\omega)\}$,

$$l_n(t) = \frac{G(t)}{G'(t_n)(t-t_n)} = \frac{T}{\pi}\int_{-\frac{\pi}{T}}^{\frac{\pi}{T}} \varphi_n(\omega)e^{j\omega t}d\omega, \tag{2.13}$$

then $\{\varphi_n(\omega)\}$ is biorthonormal to $\{e^{j\omega t_n}\}$ in $L^2[-\frac{\pi}{T},\ \frac{\pi}{T}]$ since from Eqn. (2.12) and (2.13),

$$l_n(t_k) = \frac{T}{\pi}\int_{-\frac{\pi}{T}}^{\frac{\pi}{T}} \varphi_n(\omega)e^{j\omega t_k}d\omega = \begin{cases} 1, & n=k \\ 0, & n\neq k \end{cases} . \tag{2.14}$$

It can be shown that the set of shifted sinc functions, $\left\{\frac{\sin\frac{\pi}{T}(t-t_n)}{\frac{\pi}{T}(t-t_n)}\right\}$ is the inverse Fourier transform of $\{e^{j\omega t_n}\}$ in the interval $-\frac{\pi}{T} \leq \omega \leq \frac{\pi}{T}$. Then by the isometry property of Fourier transforms, the two set of sequences

$$\left\{\frac{G(t)}{G'(t_n)(t-t_n)}\right\} \text{ and } \left\{\frac{\sin\frac{\pi}{T}(t-t_n)}{\frac{\pi}{T}(t-t_n)}\right\} \tag{2.15}$$

are biorthonormal. The above result shows the relationship between the interpolation property of the synthesis functions and the biorthonormality between the analysis and synthesis functions.

Using the Riesz basis equation in Eqn. (2.6) with $\{e^{j\omega t_n}\}$ as the analysis functions and $\{\varphi_n(\omega)\}$ as the synthesis functions,

$$A\sum_{n=-\infty}^{\infty}\left|\left\langle X(\omega), e^{j\omega t_n}\right\rangle\right|^2 \leq \left\|\sum_{n=-\infty}^{\infty}\left\langle X(\omega), e^{j\omega t_n}\right\rangle\varphi_n(\omega)\right\|^2 \leq B\sum_{n=-\infty}^{\infty}\left|\left\langle X(\omega), e^{j\omega t_n}\right\rangle\right|^2 . \tag{2.16}$$

By inverse Fourier transformation,

$$A_1\sum_{n=-\infty}^{\infty}|x(t_n)|^2 \leq \left\|\sum_n x(t_n)\frac{G(t)}{G'(t_n)(t-t_n)}\right\|^2 \leq B_1\sum_{n=-\infty}^{\infty}|x(t_n)|^2 . \tag{2.17}$$

Similar to a previous argument for Riesz bases, the right inequality of Eqn. (2.17) shows that the sampling expansion is stable. The set of sample instants $\{t_n\}$ is therefore a stable sampling set, which also implies that it is a set of uniqueness. The left inequality shows that the set of sample instants is a squared-summable sequence, and it follows that $\{t_n\}$ is a set of interpolation because the samples of $x(t) \in PW_{\omega_0}$ are the set of squared-summable sequence of values.

When the signal $x(t)$ belongs to the class of functions, $PW_{\frac{\pi-\delta}{T}}$, where $0 < \delta \leq \pi$, the signal would be oversampled if the sampling density remains as $D(t_n) = \frac{\omega_0}{\pi}$. In this case, there is a weaker constraint on the sample instants. Specifically, if

$$\begin{aligned} |t_n - nT| &< \infty \\ |t_n - t_m| &> 0, \quad n \neq m, \quad n, m \in \mathbb{Z}, \end{aligned} \tag{2.18}$$

the function $x(t) \in PW_{\frac{\pi-\delta}{T}}$ can be expressed as

$$x(t) = \sum_{n=-\infty}^{\infty} x(t_n) l_n(t), \tag{2.19a}$$

where the composing functions, $\{l_n(t)\} \in PW_{\omega_0}$ are given as

$$l_n(t) = \frac{G(t)}{G'(t_n)(t - t_n)} \tag{2.19b}$$

and

$$G(t) = (t - t_0) \prod_{k=-\infty}^{\infty} \left(1 - \frac{t}{t_k}\right) \left(1 - \frac{t}{t_{-k}}\right). \tag{2.19c}$$

From the frame condition in Eqn. (2.8),

$$A_2 \left\|X(\omega)\right\|^2 \leq \sum_{n=-\infty}^{\infty} \left|\left\langle X(\omega), e^{j\omega t_n} \right\rangle\right|^2 \leq B_2 \left\|X(\omega)\right\|^2 \tag{2.20}$$

where $\{e^{j\omega t_n}\} \in L^2\left[-\frac{\pi}{T}, \frac{\pi}{T}\right]$ and $X(\omega) \in L^2\left[-\frac{\pi+\delta}{T}, \frac{\pi-\delta}{T}\right]$. By inverse Fourier transformation of Eqn. (2.20),

$$A_3 \left\|x(t)\right\|^2 \leq \sum_{n=-\infty}^{\infty} |x(t_n)|^2 \leq B_3 \left\|x(t)\right\|^2. \tag{2.21}$$

The left side of Eqn. (2.21) indicates that the sample instants $\{t_n\}$ are a set of stable samples. However, $\{t_n\}$ is not a set of interpolation for PW_{ω_0} since the density condition in Eqn. (2.3b) is not satisfied. Given any set of squared-summable sequence of values, $\{a_n\}$, the corresponding moment problem $f(t_n) = a_n$ does not give a $f(t)$ that necessarily belongs to $PW_{\frac{\pi-\delta}{T}}$.

In summary, given the condition on the sample instants in Eqn. (2.10), signals that are band-limited to π/T rad/s can be recovered from their samples using the Lagrange

interpolation functions. Signals that are band-limited to less than π/T rad/s can also be recovered using the Lagrange interpolation functions if the condition on the sample instants is as described in Eqn. (2.18).

2.4 System Interpretation of Lagrange Interpolation Function

In considering the use of Eqns. (2.9) and (2.11) for implementing the interpolation of non-uniform samples, we can form the interpolating kernel, $l_n(t)$ and apply Eqn. (2.9) to the non-uniform samples. An alternative is also suggested in [23] by noting that Eqn. (2.9) and (2.11) can equivalently be expressed as

$$x(t) = G(t) \cdot \left[\left(\sum_{n=-\infty}^{\infty} a_n \delta(t - t_n) \right) * \frac{1}{t} \right] \tag{2.22a}$$

where

$$a_n = \frac{x(t_n)}{G'(t_n)} \, . \tag{2.22b}$$

In this interpretation, the stream of samples is pre-weighted using Eqn. (2.22b), processed with a scaled Hilbert transformer and then modulated with $G(t)$. Fig. 2-2 shows the block diagram for non-uniform sampling followed by reconstruction using Eqns. (2.22).

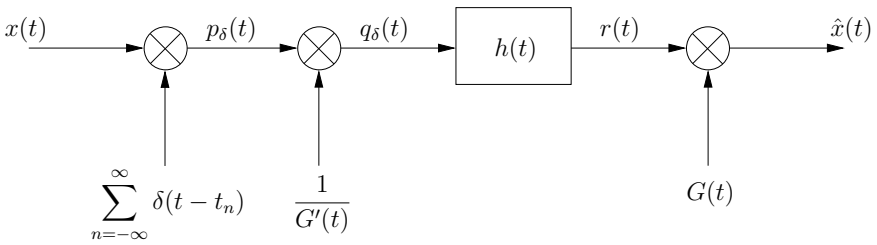

Figure 2-2: Lagrange interpolation reconstruction system

The filter, $h(t)$ has impulse response

$$h(t) = \frac{1}{t} \tag{2.23a}$$

and its corresponding frequency response is

$$H(j\Omega) = -j\pi \text{sgn}(\Omega) \tag{2.23b}$$

where

$$\text{sgn}(\Omega) = \begin{cases} -1 & ,\Omega < 0 \\ 0 & ,\Omega = 0 \\ 1 & ,\Omega > 0 \end{cases} . \tag{2.23c}$$

Due to its singularity at $t = 0$ and infinite impulse response, exact implementation of the ideal Hilbert transformer is not practical. Analog and digital implementations of the Hilbert transformer can be found in [25] and [12].

There are potential advantages with the implementation of the Lagrange reconstruction formula using Eqns. (2.22a) and (2.22b). One important advantage is that $G(t)$ only needs to be generated once in contrast to computing a set of interpolation kernels, $l_n(t)$, though in both interpretations, the key dependence is on $G(t)$. Another potential advantage of the system shown in Fig. 2-2 is that the separate components within the system can be varied to form approximations to the Lagrange interpolation formula. These two advantages will be exploited in the subsequent chapters of this thesis.

2.4.1 Frequency domain interpretation

In this section, we show with a simple example the interpretation of Fig. 2-2 for the special case of uniform sampling by demonstrating in the frequency domain.

Fig. 2-3(a) illustrates the Fourier transform of a bandlimited continuous-time signal $x(t)$. The signal is uniformly sampled at times $t_n = nT$,

$$\begin{aligned} p_\delta(t) &= x(t) \sum_{n=-\infty}^{\infty} \delta(t - t_n) \\ &= \sum_{n=-\infty}^{\infty} x(nT)\delta(t - nT) \ . \end{aligned} \tag{2.24}$$

The Fourier transform of $p_\delta(t)$ is a periodic replication of the spectrum $X(j\Omega)$ with a period of $2\pi/T$ as shown in Fig. 2-3(b). For the case of uniform sampling, the function $G(t)$ is

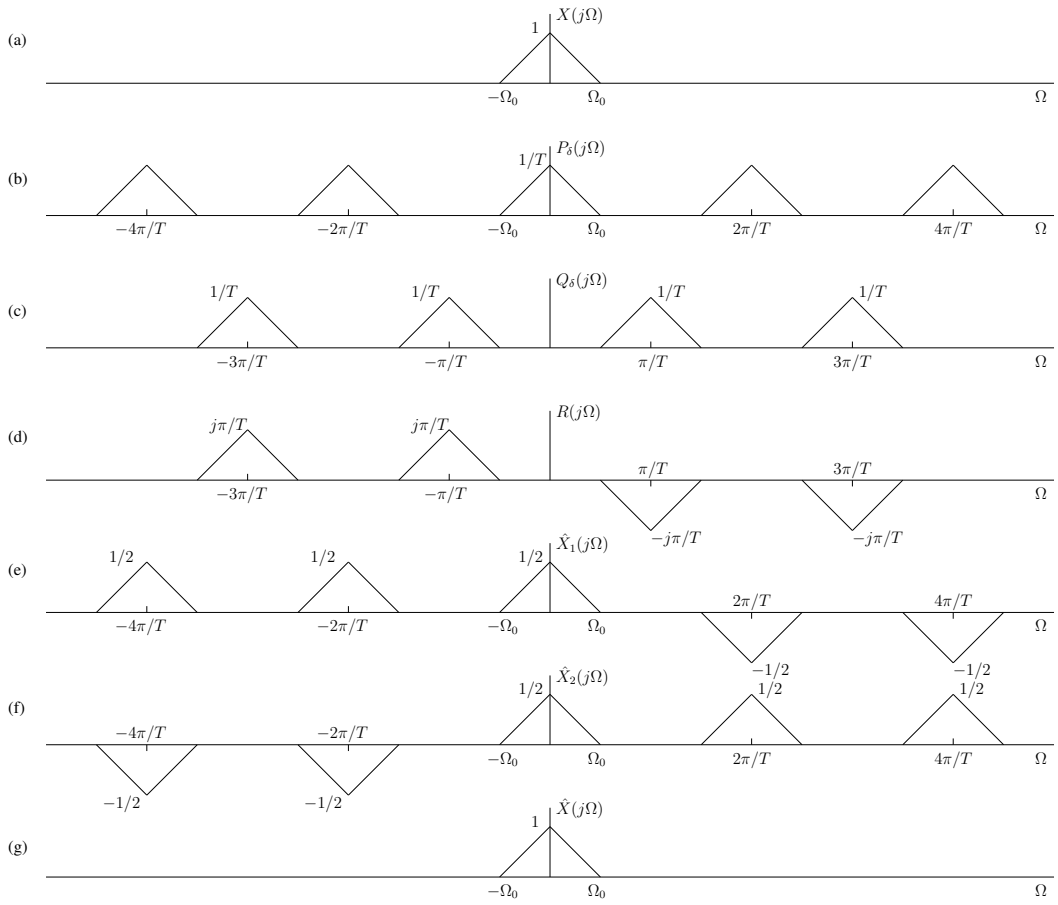

Figure 2-3: Frequency domain plots for the Lagrange reconstruction system

given by

$$G(t) = \frac{\sin(\pi t/T)}{\pi/T} \tag{2.25}$$

which has all its zeros at the sampling locations. The first derivative of $G(t)$ is

$$G'(t) = \cos(\pi t/T)\ . \tag{2.26}$$

The sequence $p_\delta(t)$ is then multiplied with $1/G'(t)$ to obtain the input $q_\delta(t)$ of the Hilbert

transformer as

$$\begin{aligned} q_\delta(t) &= \frac{1}{\cos(\pi t/T)} \sum_{n=-\infty}^{\infty} x(nT)\delta(t-nT) \\ &= \sum_{n=-\infty}^{\infty} x(nT)\frac{\delta(t-nT)}{\cos(n\pi)} \\ &= \sum_{n=-\infty}^{\infty} x(nT)\frac{\delta(t-nT)}{(-1)^n} \\ &= \sum_{n=-\infty}^{\infty} x(nT)\delta(t-nT)(-1)^n \ . \end{aligned} \tag{2.27}$$

This is equivalent to modulating $p_\delta(t)$ by $\cos(n\pi)$, which corresponds to shifting by π/T in the frequency domain as shown in Fig. 2-3(c). When the signal $q_\delta(t)$ is passed through the Hilbert transformer, the output is

$$\begin{aligned} r(t) &= \int_{-\infty}^{\infty} \sum_{n=-\infty}^{\infty} x(nT)\cos(n\pi)\delta(\tau-nT)\cdot \frac{1}{t-\tau} d\tau \\ &= \sum_{n=-\infty}^{\infty} x(nT)\frac{\cos(n\pi)}{t-nT} \ . \end{aligned} \tag{2.28}$$

Fig. 2-3(d) shows the output of the Hilbert transformer, which can be obtained by multiplying Fig. 2-3(c) with the frequency response of the Hilbert transformer given by Eqns. (2.23). The last procedure of the Lagrange interpolating system is to modulate $r(t)$ by $G(t)$.

$$\begin{aligned} \hat{x}(t) &= \sum_{n=-\infty}^{\infty} x(nT)\frac{\sin(\pi t/T)\cos(n\pi)}{\frac{\pi}{T}(t-nT)} \\ &= \sum_{n=-\infty}^{\infty} x(nT)\frac{\sin(\frac{\pi}{T}(t-nT))}{\frac{\pi}{T}(t-nT)} \ . \end{aligned} \tag{2.29}$$

This last step can be described as aliasing cancellation since it can be seen from Figs. 2-3(e) and 2-3(f) that the two complex exponential parts of the sine function, $G(t)$ will modulate $r(t)$ by π/T and $-\pi/T$ respectively. Their difference would cancel the replications, thus

leaving the baseband portion which is the reconstructed signal spectrum.

$$\begin{aligned} \hat{x}(t) &= r(t) \cdot \frac{\sin(\pi t/T)}{\frac{\pi}{T}} \\ &= \frac{r(t)e^{j\pi t/T} - r(t)e^{-j\pi t/T}}{j2\frac{\pi}{T}} \\ &= \hat{x}_1(t) + \hat{x}_2(t) \ . \end{aligned} \tag{2.30}$$

The above frequency domain interpretation of the Lagrange interpolation system suggests that instead of interpreting of the time domain sinc function simply as a rectangular low-pass filter in the frequency domain in the case of uniformly spaced samples, we can view the interpolation with the sinc function as an aliasing cancellation operation for the case of uniformly spaced samples.

Chapter 3

Time-Warping in Non-uniform Sampling

In this chapter, we represent non-uniform sampling of signals using time-warping. Delay modulation is formulated as an interpretation of time-warping to describe non-uniform sampling, specifically in the context where the sample instants are bounded deviations from a known uniform grid, as defined in section 2 of this chapter. Possible techniques for obtaining the inverse warping operator are examined. A discussion is also made about two-dimensional input-output representations of delay modulation. The last section in this chapter discusses approximations of the delay modulation function in various non-uniform sampling problems.

3.1 Interpretation of Time-warping

Time-warping is the transformation of a signal through the distortion of the time-axis. This can be described by the mapping

$$t = \beta(u) \tag{3.1}$$

where the warping operator, β is a function of the input time, u and obtains the output time, t such that $t = \beta(u)$. In non-uniform sampling and reconstruction of signals, time-warping can be applied in various ways throughout the entire process. In general, there are two approaches to relate time-warping to the context of non-uniform sampling.

One approach is to interpret a non-uniform sampling problem as uniform sampling of a

time-warped signal, which is discussed in [22]. The initial band-limited signal is warped in such a manner that the uniform sample values of the warped signal are equivalent to the values obtained through non-uniform sampling of the pre-warped signal. In this case, the samples lie on the uniform grid of the warped time-axis, and the samples can be interpolated using the sinc kernel, which achieves the interpolation property on the uniform grid. The reconstructed signal is then obtained by inverse warping the interpolated signal. However, this process does not lead to perfect reconstruction of the signal since the post-warped signal is non-bandlimited and sampling it uniformly would cause aliasing.

The warping function can also be used to warp the analysis and synthesis kernels. This can be done when the kernels do not have a computationally simple expression. Time-warping of simple and analytically well-defined functions allows for the creation of an extensive set of kernels with complicated functions that satisfy certain properties. An example is to warp the sine function such that its zeros coincide with the sample instants, and this creates a kernel which fulfills the interpolation property. It will be shown later in chapter 4 that the component $G(t)$ of the Lagrange kernel can be modelled by a modulated warped sine function.

3.1.1 Advantages and limitations of time-warping

Time-warping can be used to represent time-varying processes such as the Lagrange kernel, which is used for reconstructing band-limited signals from non-uniform samples. These time-varying processes are transformed by time-warping so that time-invariant operations such as low-pass filtering could be used instead.

Time-warping operators can be constructed as unitary operators, where the inverse operator is identical to its adjoint. The property gained from unitary operators is that they preserve the inner products of warped functions such that

$$\langle Ax, Ay \rangle = \langle x, y \rangle \tag{3.2}$$

where A is a unitary time-warping operator. Hence, time-warping a set of orthonormal functions using unitary operators results in the set of warped functions being orthonormal as well [4]. This provides the ability to warp the orthonormal basis functions of a subspace in L^2 to form another set of orthonormal basis functions that spans a different or warped

subspace in L^2.

There are also some limitations of time-warping. As the warping operator is invertible, i.e. both onto and one-to-one, the warping functions have to be continuous and monotonically increasing. The latter condition limits the range of functions that a warping operator can map to. Since unitary time-warping operators are invertible, it is necessary that they are both continuous and monotonically increasing.

Another limitation of time-warping is that not all functions can be obtained by time-warping a given function, as there might be a case where the dynamic range of the pre-warped signal is not a subset of the dynamic range of the desired signal. Similar to the limitation for monotonically increasing warping functions, there is a constraint on the range space of warping operators.

3.2 Formulation of Delay-modulation Method

In this section, an alternative interpretation of time-warping of signals is introduced. The notion here is that time-warping of signals can be expressed as a time-varying time-shift such that

$$\beta(t) = t - \alpha(t)\,. \tag{3.3}$$

This is also known as delay-modulation in communications theory [4], [35]. Delay modulation is an alternative way of relating time-warping to non-uniform sampling, especially in the context where the sample instants t_n are deviations from a uniform grid with spacing T, i.e.,

$$t_n = nT + \epsilon_n \tag{3.4}$$

where the set $\{\epsilon_n\}$ contains the deviations of the sampling instants away from the uniform grid.

One way of representing delay modulation is by modeling it as a linear time-varying (LTV) system,

$$h(t,u) = \delta\left(t - u - \alpha(t)\right) \tag{3.5}$$

where t is the observation (output) time and u is the excitation (input) time. The impulse response is completely characterized by the output time-dependent delay function $\alpha(t)$. The superposition of the input signal, $x(t)$ with the LTV system causes a time-dependent shift

of $x(\cdot)$ to obtain the warped signal

$$\begin{aligned} y(t) &= \int_{-\infty}^{\infty} h\left(t,u\right) x(u)\mathrm{d}u \\ &= \int_{-\infty}^{\infty} \delta\left(t-u-\alpha(t)\right) x(u)\mathrm{d}u \\ &= x\left(t-\alpha(t)\right) \ . \end{aligned} \tag{3.6}$$

Though the delay function $\alpha(t)$ does not necessarily have to satisfy any constraints, $\beta(t)$ in Eqn. (3.3) can be restricted to be continuous and monotonic so that the warping function is invertible. Therefore, $0 < \beta'(t) < \infty$ and so $-\infty < \alpha'(t) < 1$.

3.3 Determining the Inverse Warping System

The aim of this section is to examine possible techniques for obtaining the inverse warping operator. We move beyond the constraint of requiring the warping functions to be monotonically increasing while retaining the continuity constraint. Two different possible expressions for the inverse warping function will be discussed. Throughout this section, the forward warping operator has the impulse response as given in Eqn. (3.5).

3.3.1 Approach 1: Using the substitution of variables

The first approach uses a substitution of variables method to obtain the output of the inverse system. The impulse response of the inverse system can be defined as

$$h_1(t,u) = \beta'(u)\delta(t-\beta(u)), \tag{3.7}$$

where $\beta(u) = u - \alpha(u)$, and $\beta'(u)$ is the first derivative of $\beta(u)$ with respect to u.

The output of the inverse system is

$$\begin{aligned} \hat{x}(t) &= \int_{-\infty}^{\infty} h_1(t,u)y(u)\mathrm{d}u \\ &= \int_{-\infty}^{\infty} \beta'(u)\delta\left(t-\beta(u)\right) y(u)\mathrm{d}u. \end{aligned} \tag{3.8}$$

Let $\phi = \beta(u)$, and its derivative with respect to u is

$$\frac{\mathrm{d}\phi}{\mathrm{d}u} = \beta'(u). \tag{3.9}$$

By making a substitution of variables on Eqn. (3.8), the output of the inverse system is

$$\begin{aligned}
\hat{x}(t) &= \int_{-\infty}^{\infty} \beta'(u)\delta(t-\phi)y(\beta^{-1}(\phi))\frac{1}{\beta'(u)}\mathrm{d}\phi \\
&= \int_{-\infty}^{\infty} \delta(t-\phi)y(\beta^{-1}(\phi))\mathrm{d}\phi \\
&= y(\beta^{-1}(t)) \\
&= x(\beta(\beta^{-1}(t))) \\
&= x(t)\ .
\end{aligned} \tag{3.10}$$

From Eqn. (3.10), we see that the scaling factor $\beta'(u)$ in Eqn. (3.7) normalizes the output of the inverse warping operation to obtain a unity gain through the warping and inverse warping processes. If the warping function $\beta(\cdot)$ is monotonically increasing, it is possible to obtain the output of the inverse system as $x(t)$. However, this formulation of the inverse system would not hold for intervals where $\beta'(\cdot) \leq 0$, since $\beta(\cdot)$ is not one-to-one and so $\beta^{-1}(\cdot)$ will not be a valid function. Therefore, the second line of Eqn. (3.10) is invalid when $\beta(\cdot)$ is not one-to-one. At the stationary points of the warping function, which are instants where $\beta'(\cdot) = 0$, the impulse response $h_1(t,u)$ is zero. This is equivalent to $\alpha'(\cdot) = 1$, which means that when the rate of the delay is the same as the rate of the time, the output value of the inverse system would be zero. For warping functions with $\beta'(\cdot) \geq 0$, one way of overcoming this zero output at the instance where $\alpha'(\cdot) = 1$, is to use the continuity of the signal to interpolate the value.

Clearly, this inverse warping operator is only suitable for monotonically increasing warping functions. The next approach aims to obtain an inverse warping operator which could also be extended to non-monotonically increasing functions.

3.3.2 Approach 2: Using the generalized scaling property of the Dirac delta function

The second approach to finding the inverse warping is to use the generalized scaling property of Dirac delta functions,

$$\delta(p(x)) = \sum_i \frac{\delta(x - x_i)}{|p'(x_i)|} \tag{3.11}$$

where x_i are the roots of the scaling function, $p(x)$ and i represents the root indices.

Similar to the first approach, the impulse response of the inverse system is defined as

$$h_2(t, u) = |\beta'(u)|\delta(t - \beta(u)) \; . \tag{3.12}$$

In this impulse response, the normalizing function is the absolute value of $\beta'(u)$ and so $|\beta'(\cdot)| \geq 0$. The output of the reverse system is

$$\begin{aligned}
\hat{x}(t) &= \int_{-\infty}^{\infty} h_2(t, u) y(u) \mathrm{d}u \\
&= \int_{-\infty}^{\infty} |\beta'(u)| \delta\left(t - \beta(u)\right) y(u) \mathrm{d}u \\
&= \int_{-\infty}^{\infty} |\beta'(u)| y(u) \sum_i \frac{\delta\left(u - u_i\right)}{|\beta'(u_i)|} \mathrm{d}u \\
&= \sum_i \frac{|\beta'(u_i)| y(u_i)}{|\beta'(u_i)|} \\
&= \sum_i y(u_i) \\
&= \sum_i x(\beta(u_i)) \\
&= ix(t), \quad \text{where } \; i = \#(\text{roots of } t = \beta(u_i)).
\end{aligned} \tag{3.13}$$

Since the roots u_i are the values of u when the polynomial $p(u) = t - \beta(u)$ equals to zero, this means that at the instants, u_i, $\beta(u_i) = t$. When the function $\beta(u)$ is not monotonic, there is the possibility that multiple roots can occur for particular values of t. This introduces a scaling factor for certain intervals of the warping function. Therefore, a region of the inversed warped signal is scaled by the number of roots present in $\beta(u)$ for that region of t. We can illustrate this with a pictorial representation in Fig. 3-1, which shows a non-monotonically increasing warping function $\beta(u)$. If the intervals of t where the warping function has multiple roots are known, it is possible to recover $x(t)$ by re-scaling those

regions of the inverse warped signal.

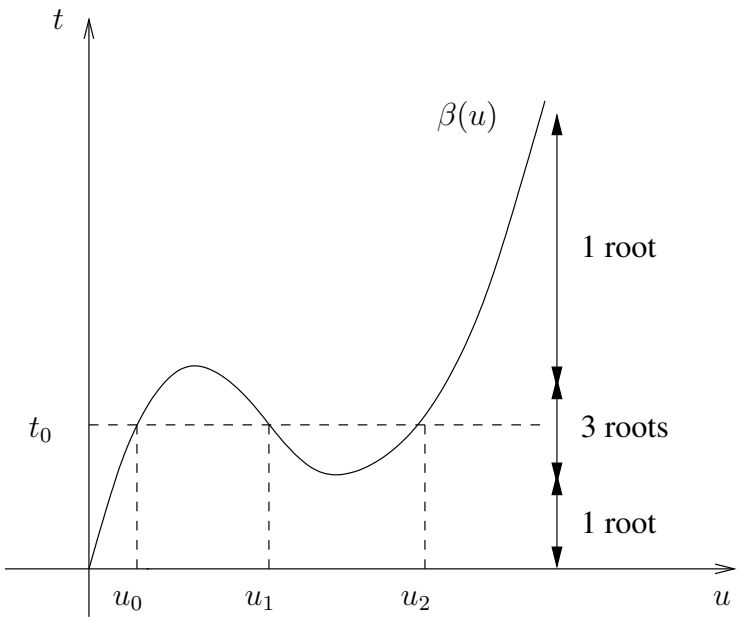

Figure 3-1: Example of non-monotonic warping function.

3.4 Delay Modulation Representation of Non-uniform Sampling

An interpretation of non-uniform sampling using delay modulation is presented in this section. Specifically, delay modulation is used to represent the case of non-uniform sampling where the sampling instants deviate from a uniform grid, as described in Eqn. (3.4). In the first part of this section, we will impose constraints on the warping functions to ensure that the non-uniform sample instants map to the uniform grid and vice-versa. The second part of this section then shows how non-uniform sampling can be interpreted as a process of inverse-warping a signal, uniform sampling of the inversed warped signal and warping the output stream of samples.

The non-uniform sample instants, t_n, can be characterized as uniform samples of an inverse warping function $\beta^{-1}(t)$ such that it satisfies the properties

$$\begin{aligned} \beta^{-1}(nT) &= t_n \ , \\ \beta(t_n) &= nT \ , \quad \forall n \in \mathbb{Z} \ . \end{aligned} \tag{3.14}$$

If $\beta^{-1}(t)$ is expressed in terms of delay modulation such that $\beta^{-1}(t) = t + \epsilon(t)$, then Eqn. (3.14) gives

$$\begin{aligned} \beta^{-1}(nT) &= t_n \\ nT + \epsilon(nT) &= nT + \epsilon_n \\ \epsilon(nT) &= \epsilon_n \ . \end{aligned} \tag{3.15}$$

where the deviations, ϵ_n, are expressed as the uniform samples of the delay modulation function, $\epsilon(t)$. Similarly, by expressing the forward warping function as $\beta(t) = t - \alpha(t)$, the deviations ϵ_n are characterized by $\alpha(t)$ such that

$$\begin{aligned} \beta(t_n) &= nT \\ t_n - \alpha(t_n) &= nT \\ \alpha(t_n) &= \epsilon_n \ . \end{aligned} \tag{3.16}$$

The constraint given in Eqn. (3.16) ensures that the delay modulation function maps the non-uniform sample instants, t_n, onto the uniform grid. An additional constraint of $-\infty < \alpha'(t) < 1$ ensures that the warping function is invertible. Unless the class of functions which $\alpha(t)$ belongs to is known, $\alpha(t)$ is not uniquely defined.

Non-uniform sampling can be viewed as a process of inverse warping the signal, uniformly sampling it, and warping the output stream of samples. An illustration of this process is shown in Fig. 3-2. We define the inverse warping operator C^{-1} to have the impulse response given in Eqn. (3.7) while the impulse response of the warping operator, C is given by Eqn. (3.5). Inverse time-warping the signal $x(t)$ followed by uniform sampling gives

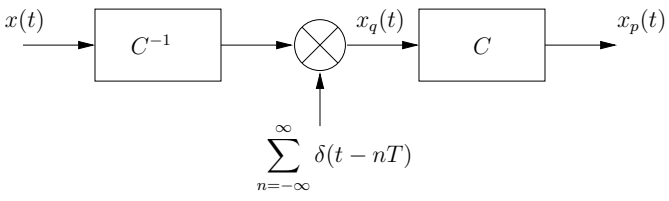

Figure 3-2: Equivalent non-uniform sampling using time-warping.

$$
\begin{aligned}
x_q(t) &= x(\beta^{-1}(t)) \sum_{n=-\infty}^{\infty} \delta(t - nT) \\
&= \sum_{n=-\infty}^{\infty} x(t_n)\delta(t - nT) \ , \qquad (3.17)
\end{aligned}
$$

where the non-uniform sample values are located on the uniform grid. The signal $x_q(t)$ can then be warped with $\beta(t)$ to map the sample values onto the non-uniform grid such that

$$
\begin{aligned}
x_p(t) = x_q(\beta(t)) &= \sum_{n=-\infty}^{\infty} x(t_n)\delta(\beta(t) - nT) \\
&= \sum_{n=-\infty}^{\infty} x(t_n)\delta(t - t_n) \ . \qquad (3.18)
\end{aligned}
$$

Similarly, uniform sampling is represented as warping the signal, followed by non-uniform sampling and an inverse warping of the output. This process is illustrated in Fig. 3-3 .

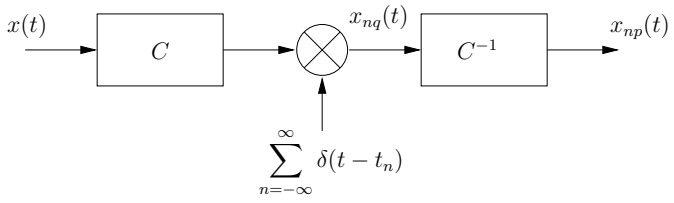

Figure 3-3: Equivalent uniform sampling using time-warping.

3.5 Two-dimensional Representation of Delay Modulation

In this section, we introduce different input-output system characterizations of delay modulation. These characterizations allow us to describe the effects of sampling the warped signal and show what this means in terms of the input system.

The time-varying impulse response, $h(t, u)$ given in Eqn. (3.5) gives the relationship between the input signal and output signal in terms of input time, u and output time, t. This time-domain relationship as expressed in Eqn. (3.6), can be re-written by replacing u

with $u - \alpha(t)$,

$$\begin{aligned} y(t) &= \int_{-\infty}^{\infty} h(t, u-\alpha(t))x(u-\alpha(t))\mathrm{d}u \\ &= \int_{-\infty}^{\infty} \delta(t-\alpha(t)-(u-\alpha(t)))x(u-\alpha(t))\mathrm{d}u \\ &= \int_{-\infty}^{\infty} \delta(t-u)x(u-\alpha(t))\mathrm{d}u\ . \end{aligned} \tag{3.19}$$

We can represent Eqn. (3.19) in two-dimensions as shown in Fig. 3.5. The input signal can be seen as being laid out at each instance of t, and shifted by an amount $\alpha(t)$ which depends on the observation time, t. For example, at time $t = t_0$, the signal is shifted by an amount $\alpha(t_0)$. The output, $y(t)$ of the LTV system can be obtained from Eqn. (3.19), by evaluating the shifted two-dimensional signal along the diagonal line representing $u = t$.

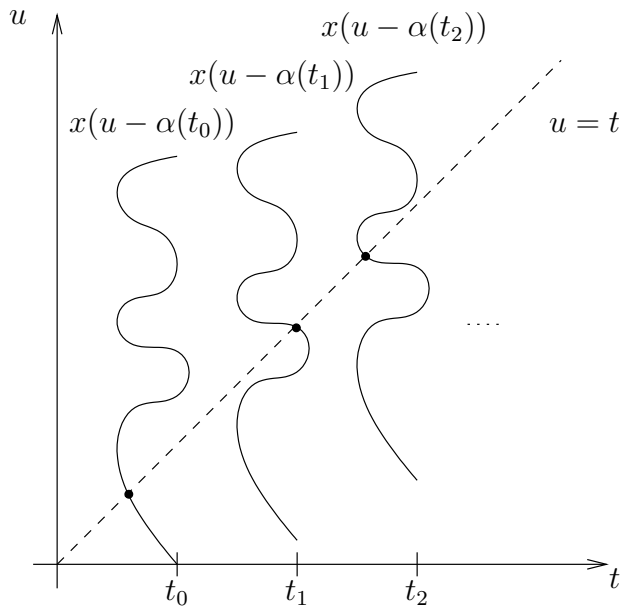

Figure 3-4: Two-dimensional input time - output time representation of delay modulation.

The time-warping operator can also be characterized in terms of the input frequency

and the output frequency. The Fourier transform of the output signal is

$$\begin{aligned} Y(\Omega) &= \int_{-\infty}^{\infty} y(t) e^{-j\Omega t} \mathrm{d}t \\ &= \int_{-\infty}^{\infty} \left[\frac{1}{2\pi} \int_{-\pi}^{\pi} X(\omega) e^{j\omega u} \mathrm{d}\omega \right] e^{-j\Omega t} \mathrm{d}t \\ &= \frac{1}{2\pi} \int_{-\pi}^{\pi} \left[\int_{-\infty}^{\infty} e^{j\omega(t-\alpha(t))} e^{-j\Omega t} \mathrm{d}t \right] X(\omega) \mathrm{d}\omega \\ &= \frac{1}{2\pi} \int_{-\pi}^{\pi} H(\Omega, \omega) X(\omega) \mathrm{d}\omega \end{aligned} \tag{3.20}$$

where the bi-frequency transfer function $H(\Omega, \omega)$ can be obtained by the two-dimensional Fourier transform of $h(t, u)$,

$$\begin{aligned} H(\Omega, \omega) &= \int_{-\infty}^{\infty} \int_{-\infty}^{\infty} h(t, u) e^{j\omega u} e^{-j\Omega t} \mathrm{d}u \, \mathrm{d}t \\ &= \int_{-\infty}^{\infty} \int_{-\infty}^{\infty} \delta(t - u - \alpha(t)) e^{j\omega u} e^{-j\Omega t} \mathrm{d}u \, \mathrm{d}t \\ &= \int_{-\infty}^{\infty} e^{j\omega(t-\alpha(t))} e^{-j\Omega t} \mathrm{d}t \, . \end{aligned} \tag{3.21}$$

The third characterization is the input frequency to output time representation of the time-varying system. Substituting the expression for the inverse Fourier transform of $x(u)$ into Eqn. (3.6),

$$\begin{aligned} y(t) &= \int_{-\infty}^{\infty} h\,(t, u) \left[\frac{1}{2\pi} \int_{-\pi}^{\pi} X(\omega) e^{j\omega u} \mathrm{d}\omega \right] \mathrm{d}u \\ &= \frac{1}{2\pi} \int_{-\pi}^{\pi} \left[\int_{-\infty}^{\infty} h\,(t, u)\, e^{j\omega u} \mathrm{d}u \right] X(\omega) \mathrm{d}\omega \\ &= \frac{1}{2\pi} \int_{-\pi}^{\pi} g(t, \omega) X(\omega) \mathrm{d}\omega \end{aligned} \tag{3.22}$$

where the input frequency and output time response function

$$\begin{aligned} g(t, \omega) &= \int_{-\infty}^{\infty} h\,(t, u)\, e^{j\omega u} \mathrm{d}u \\ &= \int_{-\infty}^{\infty} \delta(t - u - \alpha(t)) e^{j\omega u} \mathrm{d}u \\ &= e^{j\omega(t-\alpha(t))} \, . \end{aligned} \tag{3.23}$$

By combining Eqn. (3.23) and Eqn. (3.22), $y(t)$ can be expressed as

$$y(t) = \frac{1}{2\pi} \int_{-\pi}^{\pi} X(\omega) e^{-j\omega\alpha(t)} e^{j\omega t} \mathrm{d}\omega \tag{3.24}$$

which can be interpreted as $y(t)$ being the projection of $\tilde{X}(t,\omega) = g(t,\omega)X(\omega)$ onto the t-axis. We can visualize this as laying out the signal $x(u)$ for different time instants, t, and carrying out the one-dimensional Fourier Transform along the u-axis to obtain $X(\omega)$. Subsequently at each instant of observation time, t, $X(\omega)$ is multiplied with a phase shift of $e^{-j\omega\alpha(t)}$. The above perspective of delay modulation method allows an easier understanding of time-warping of the signal.

3.6 Approximations of Time-warped Signals

This section explores the idea of making approximations involving the warping function. The first part of the section uses the non-uniform sample instants, t_n to obtain approximations of the delay modulation, $\epsilon(t)$. The second part then assumes that $\epsilon(t)$ is known and uses the original signal and the warping function to form approximations to the frequency spectrum of the warped function.

3.6.1 Approximation of time-warping functions

In this first part, we discuss how the inverse time-warping functions, $\beta^{-1}(t) = t + \epsilon(t)$ can be approximated from non-uniform sampling instants, specifically for the cases of bounded deviation from the uniform grid and recurrent non-uniform sampling.

In considering the case where the sample instants t_n deviate from the uniform grid by a bounded amount, we can represent the deviations ϵ_n with a delay modulation function $\epsilon(t)$. One method of forming $\epsilon(t)$ is to use a series expansion

$$\epsilon(t) = \sum_{n=-\infty}^{\infty} \epsilon_n \phi_n(t), \tag{3.25}$$

where the set of functions $\{\phi_n(t)\}$ are either bases or frames that span the space which $\epsilon(t)$ belongs to. This space is unknown in most cases and we can use the characteristics of t_n to form approximations of $\epsilon(t)$. An example is to approximate $\epsilon(t)$ while satisfying the condition in Eqn. (3.15), and hence it is sufficient for the approximation scheme to

fulfill the interpolation property. By approximating $\epsilon(t)$ to belong to the space of functions band-limited to $\frac{\pi}{T}$, we can express

$$\epsilon(t) = \sum_{n=-\infty}^{\infty} \epsilon_n \frac{\sin \frac{\pi}{T}(t - nT)}{\frac{\pi}{T}(t - nT)}. \tag{3.26}$$

Another similar method to obtain $\epsilon(t)$, while satisfying the condition in Eqn. (3.15), uses uniform splines to interpolate the deviations ϵ_n.

For the case of recurrent non-uniform sampling, the delay modulation function can be described as a periodic function. An example would be to approximate the delay modulation function with trigonometric polynomials as described in the following discussion. Assume that the sample instants are divided into groups of N points each and the groups have a recurrent period of T_Q, which is N times the Nyquist period, T. Each period consists of N non-uniform sample instants which are denoted by t_p, $p = 0, 1, \ldots, N-1$. The complete set of sample instants are $t_p + nT_Q$, $p = 0, 1, \ldots, N-1$, $n \in \mathbb{Z}$. The delay modulation function, $\epsilon(t)$ can be sufficiently described as a real and periodic function with period, T_Q such that

$$\epsilon(nT_Q + pT) = \epsilon((n+1)T_Q + pT) = t_p, \quad p = 0, 1, \ldots, N-1, \tag{3.27}$$

and therefore, $\epsilon(t)$ can be expressed as a Fourier series

$$\epsilon(t) = a_0 + \sum_{k=1}^{\infty} \left[a_k \cos\left(k \frac{2\pi}{T_Q} t\right) + b_k \sin\left(k \frac{2\pi}{T_Q} t\right) \right]. \tag{3.28}$$

However, $\epsilon(t)$ is unknown and we want to approximate it from the sample instants. The first N Fourier series coefficients of Eqn. (3.28) can be approximated from the sample instants, t_p, $p = 0, 1, \ldots, N-1$ by solving the system of equations

$$\epsilon(pT) = t_p = a_0 + \sum_{k=1}^{\frac{N-1}{2}} \left[a_k \cos\left(k \frac{2\pi}{T_Q} pT\right) + b_k \sin\left(k \frac{2\pi}{T_Q} pT\right) \right], \quad p = 0, 1, \ldots, N-1. \tag{3.29}$$

This results in the approximation of $\epsilon(t)$ with N trigonometric polynomial terms.

In some other cases such as in polynomial-based frequency modulation, $\epsilon(t)$ may be

approximated using a Taylor series expansion

$$\epsilon(t) = a_0 + a_1 t + a_2 t^2 + \dots . \tag{3.30}$$

However, if the Taylor series approximation is to be used for the special case of non-uniform sampling where the sample instants are deviations from a uniform grid, then we have to also consider the constraints given by the sample instants. For example, in the case where the deviations from the uniform grid are less than 1/4 of the average sampling period, it is sufficient to expect that $\epsilon(t)$ is bounded. However, a truncation of the Taylor series expansion for $\epsilon(t)$ would result in higher order terms which would contradict the boundedness condition for $\epsilon(t)$.

3.6.2 Frequency representation of warped functions

Assume that $x(t)$ has a Fourier transform $X(\Omega)$ with a band-width of $\frac{\pi}{T}$. Since the warped function is expressed as an implicit function, it is generally difficult to express a warped function in terms of its Fourier transform. An approximation of the Fourier transform can be made through a Taylor series expansion of the time-warped signal such that

$$x(t+\epsilon(t)) = x(t) + \epsilon(t)x'(t) + \epsilon^2(t)\frac{x''(t)}{2!} + \dots + \epsilon^k(t)\frac{x^{(k)}(t)}{k!} + \dots \tag{3.31}$$

The Taylor series expansion in Eqn. (3.31) shows that the impact of the k^{th} term diminishes with $\frac{1}{k!}$. A first order approximation of the Fourier transform of $x(t+\epsilon(t))$ is

$$X(\Omega) + [j\Omega X(\Omega)] * E(\Omega) \ . \tag{3.32}$$

The convolution of a band-limited spectrum $X(\Omega)$ with $E(\Omega)$ implies that the Fourier transform of $x(t+\epsilon(t))$ is not band-limited to $\frac{\pi}{T}$.

Higher approximations show that, in general, the Fourier transform of $x(t+\epsilon(t))$ is not band-limited. Assume that $\epsilon(t)$ has a Fourier transform $E(\Omega)$ which is band-limited to $\frac{\pi}{T}$ and let $E = \max_\Omega |E(\Omega)|$. $E(\Omega)$ is therefore bounded by a rectangle, $R_E(\Omega)$ of support $\frac{2\pi}{T}$ and height E. The Fourier transform of the k^{th} term in Eqn. (3.31) is

$$\frac{(j\Omega)^k}{k!} X(\Omega) * E(\Omega) * \dots * E(\Omega) \tag{3.33}$$

where the dots represent a k-fold convolution of $E(\Omega)$, and the expression in Eqn. (3.33) is bounded by

$$\frac{(j\Omega)^k}{k!} X(\Omega) * R_E(\Omega) * \cdots * R_E(\Omega) \; . \tag{3.34}$$

From [28], it is shown that the k-fold convolution of $R_E(\Omega)$ converges to a Gaussian function as k tends to infinity. This implies that the Fourier transform of $\epsilon^k(t)$ is bounded by

$$|\mathcal{FT}\{\epsilon^k(t)\}| \leq \frac{E^k}{\sqrt{\frac{\pi(k+1)}{6}}} \cdot e^{-\frac{6T^2}{\pi^2(k+1)}\Omega^2} . \tag{3.35}$$

where $\mathcal{FT}\{\cdot\}$ represents a Fourier transform. The above analysis shows that the Fourier transform of $x(t+\epsilon(t))$ is in general not band-limited and the Fourier transform is bounded by a function that approximately decays like a Gaussian function.

We can also look at the Fourier transform of the warping function in another perspective. By considering the Fourier transform of $y(t) = x(\beta(t))$,

$$\begin{aligned} Y(\Omega) &= \int_{-\infty}^{\infty} y(t) e^{-j\Omega t} dt \\ &= \int_{-\infty}^{\infty} x(\beta(t)) e^{-j\Omega t} dt \; . \end{aligned} \tag{3.36}$$

Let $\tau = \beta(t)$ and $\beta^{-1}(t) = t + \epsilon(t)$. Eqn. (3.36) becomes

$$\begin{aligned} Y(\Omega) &= \int_{-\infty}^{\infty} x(\tau) \left(\frac{d\beta^{-1}(\tau)}{d\tau} \right) e^{-j\Omega\beta^{-1}(\tau)} d\tau \\ &= \int_{-\infty}^{\infty} x(\tau)(1+\epsilon'(\tau)) e^{-j\Omega\epsilon(\tau)} e^{-j\Omega\tau} d\tau \; . \end{aligned} \tag{3.37}$$

Expressing $Y(\Omega)$ in terms of convolution,

$$Y(\Omega) = X(\Omega) * [\delta(\Omega) + j\Omega E(\Omega)] * \mathcal{FT}[e^{-j\Omega\epsilon(\tau)}] \; . \tag{3.38}$$

Let us make the approximation that $\lim_{|\tau|\to\infty} \epsilon(\tau) = 0$ and that $e^{-j\Omega\epsilon(\tau)}$ can be approximated by $1 - j\Omega\epsilon(\tau)$, then the Fourier transform of $e^{-j\Omega\epsilon(\tau)}$ is

$$\begin{aligned} \int_{-\infty}^{\infty} [1 - j\Omega\epsilon(\tau)] e^{-j\Omega\tau} d\tau &= \delta(\Omega) + \epsilon(\tau) e^{-j\Omega\tau} \Big|_{-\infty}^{\infty} + \int_{-\infty}^{\infty} \epsilon'(\tau) e^{-j\Omega\tau} d\tau \\ &= \delta(\Omega) + j\Omega E(\Omega) \; . \end{aligned} \tag{3.39}$$

Combining Eqns. (3.37) and (3.39), we obtain an approximation to the Fourier transform of the warped function as

$$Y(\Omega) = X(\Omega) * [\delta(\Omega) + j\Omega E(\Omega)] * [\delta(\Omega) + j\Omega E(\Omega)] \tag{3.40}$$

which gives a similar result to that obtained through the Taylor series expansion in Eqn. (3.33).

The above analysis shows that given the Fourier transform of both $x(t)$ and $\epsilon(t)$, it is possible to obtain approximations to the Fourier transform of the warped signal through a simple convolution and sum process.

Chapter 4

Approximations to the Lagrange Interpolation Function

The reconstruction of a band-limited signal from its non-uniform samples in general involves an interpolating kernel (the Lagrange kernel) that is impractical to implement. Unlike the sinc kernel used in reconstruction from uniform samples, the kernel for the non-uniform case is computationally difficult. In this chapter, we develop approximations for the exact interpolation function to obtain efficient and accurate reconstructions. The properties of the ideal Lagrange interpolating function and its component functions will be used to specify a set of essential conditions from which we establish a framework for the approximations. Examples of approximation to Lagrange interpolation include sinc functions, piecewise sinusoids and non-uniform splines. The performance of the proposed method is then compared with direct cubic B-spline interpolation of non-uniform samples.

4.1 Characteristics of the Lagrange Interpolation Function

In this section, we study the properties of the Lagrange kernel and its components. These insights will then be used to form approximations of the Lagrange kernel that preserve its essential characteristics.

As given in Eqns. (2.11) and repeated here, for ease of reference, the equations describing

Lagrange interpolation are

$$x(t) = \sum_{n=-\infty}^{\infty} x(t_n) l_n(t) \ , \tag{4.1a}$$

where

$$l_n(t) = \frac{G(t)}{G'(t_n)(t - t_n)} \tag{4.1b}$$

and

$$G(t) = (t - t_0) \prod_{\substack{k=-\infty \\ k\neq 0}}^{\infty} \left(1 - \frac{t}{t_k}\right) \ , \tag{4.1c}$$

with the sample instants constrained to $|t_n - nT| < \frac{T}{4}$.

As described by Eqn. (4.1c), $G(t)$ consists of an infinite product of linear factors of the form $(1 - t/t_k)$, which implies that $G(t)$ is a continuous function of t since $G(t)$ is differentiable at all values of t. The constraints in both Eqn. (2.10) and (2.18) require the sample instants to be separate. Consequently, $G(t)$ can only have simple real roots at t_n and so $G'(t_n) \neq 0$.

To see how the amplitude of $G(t)$ depends on the inter-sample distance, consider an example in which a single sample instant deviates from the uniform grid. For the special case of uniformly spaced sample instants,

$$G(t) = t \prod_{\substack{k=-\infty \\ k\neq 0}}^{\infty} \left(1 - \frac{t}{kT}\right) = \frac{\sin(\frac{\pi}{T}t)}{\frac{\pi}{T}} \ , \tag{4.2}$$

where in each inter-sample interval, the extremum point magnitude is equal to the value of $G(t)$ at the arithmetic mean. We consider changes to the amplitude of $G(t)$ in the immediate interval of $[(k-1)T, (k+1)T]$, $k \in \mathbb{Z}$ when a sample instant t_k deviates from $t = kT$ by ϵ_k, where $-T/4 < \epsilon_k < 0$. From Rolle's theorem, $G(t)$ contains only one extremum point, G_{ext}, between adjacent sample instants, but the location and value of G_{ext} are difficult to determine analytically. Instead, we approximate the extremum by evaluating $G(\bar{t})$, where $\bar{t}$ denotes the arithmetic mean of the interval. $G(\bar{t})$ would appear to be a good approximation to G_{ext} because changes in the inter-sample distance cause the magnitudes of G_{ext} and $G(\bar{t})$ to change in the same direction.

From Eqn. (4.1c), we note that the factor for the zeroth sample instant has a different

form from factors involving the rest of the sample instants. Thus, the analysis below will separately consider the case for $k = 0$, and the case where k is an integer other than zero.

For the case where $k = 0$, the sample instant t_0 deviates from $t = 0$ by ϵ_0, where $-T/4 < \epsilon_0 < 0$. The factor $(t - 0)$ in Eqn. (4.2) is replaced with a factor $(t - t_0)$ to obtain

$$G(t) = \frac{\sin(\frac{\pi}{T}t)}{\frac{\pi}{T}} \cdot \frac{t - \epsilon_0}{t} \, . \tag{4.3}$$

For the larger interval, the value of $G(t)$ at the arithmetic mean, $\bar{t}_l = \frac{\epsilon_0 + T}{2}$ is

$$G(\bar{t}_l) = \frac{\cos(\frac{\pi\epsilon_0}{2T})}{\frac{\pi}{T}} \cdot \frac{T - \epsilon_0}{T + \epsilon_0} \, . \tag{4.4}$$

Thus, $G(\bar{t}_l)$ is bounded to the interval $1 < \frac{\pi}{T}G(\bar{t}_l) < \frac{5}{3}\cos(\pi/8) \approx 1.54$. The value of $G(t)$ at the arithmetic mean of the smaller interval, $\bar{t}_s = \frac{\epsilon_0 - T}{2}$ is

$$G(\bar{t}_s) = -\frac{\cos(\frac{\pi\epsilon_0}{2T})}{\frac{\pi}{T}} \cdot \frac{T + \epsilon_0}{T - \epsilon_0} \, , \tag{4.5}$$

so that $-1 < \frac{\pi}{T}G(\bar{t}_s) < -\frac{3}{5}\cos(\pi/8) \approx -0.55$. The analysis for $k = 0$ shows that $|\frac{\pi}{T}G_{ext}| > 1$ for the inter-sample interval larger than T, while $|\frac{\pi}{T}G_{ext}| < 1$ for the inter-sample interval smaller than T.

For the case when k is an integer other than zero, $t_k = kT + \epsilon_k$ and so

$$\begin{aligned} G(t) &= \frac{\sin(\frac{\pi}{T}t)}{\frac{\pi}{T}} \cdot \frac{1 - \frac{t}{kT+\epsilon_k}}{1 - \frac{t}{kT}} \\ &= \frac{\sin(\frac{\pi}{T}t)}{\frac{\pi}{T}} \cdot \frac{kT + \epsilon_k - t}{kT - t} \cdot \frac{kT}{kT + \epsilon_k} \, . \end{aligned} \tag{4.6}$$

Let $\epsilon_k = \alpha_k T$ such that $-1/4 < \alpha_k < 0$. Similar to the case of $k = 0$, we evaluate Eqn. (4.6) at the arithmetic mean of the larger interval, $\bar{t}_l = \frac{kT + \epsilon_k + (k+1)T}{2}$, which is

$$\begin{aligned} G\left(\frac{kT + \epsilon_k + (k+1)T}{2}\right) &= \frac{\sin(\frac{\pi}{2}(2k+1) + \frac{\pi\alpha_k}{2})}{\frac{\pi}{T}} \cdot \frac{\alpha_k - 1}{\alpha_k + 1} \cdot \frac{k}{k + \alpha_k} \\ &= \frac{(-1)^{k+1}\cos(\frac{\pi\alpha_k}{2})}{\frac{\pi}{T}} \cdot \frac{\alpha_k - 1}{\alpha_k + 1} \cdot \frac{k}{k + \alpha_k} \, . \end{aligned} \tag{4.7}$$

This bounds $G(\bar{t}_l)$ such that $(-1)^k < \frac{\pi}{T}G(\bar{t}_l) < (-1)^k \frac{5}{3}\cos(\pi/8)\frac{k}{k-1/4}$. The arithmetic

mean of the smaller interval, $\bar{t}_s = \frac{kT+\epsilon_k+(k-1)T}{2}$, gives a corresponding $G(t)$ as

$$G\left(\frac{kT+\epsilon_k+(k-1)T}{2}\right) = \frac{\sin(\frac{\pi}{2}(2k-1)+\frac{\pi\alpha_k}{2})}{\frac{\pi}{T}} \cdot \frac{\alpha_k+1}{\alpha_k-1} \cdot \frac{k}{k+\alpha_k}$$
$$= \frac{(-1)^k \cos(\frac{\pi\alpha_k}{2})}{\frac{\pi}{T}} \cdot \frac{\alpha_k+1}{\alpha_k-1} \cdot \frac{k}{k+\alpha_k} . \quad (4.8)$$

$G(\bar{t}_s)$ is bounded by $(-1)^{k+1} < \frac{\pi}{T}G(\bar{t}_s) < (-1)^{k+1}\frac{3}{5}\cos(\pi/8)\frac{k}{k-1/4}$.

From the above analysis, we see that for all $k \in \mathbb{Z}$, an inter-sample interval larger than T causes the magnitude of $\frac{\pi}{T}G(t)$ within that interval to be larger that 1, whereas the converse is true for inter-sample distances smaller than T. From Eqn. (4.1b), the dependence of $l_n(t)$ on $G(t)$ causes $l_n(t)$ to be similarly affected by the inter-sample distance.

Using a simple example, Fig. 4-1 illustrates how $G(t)$ changes in the interval $-T \le t \le T$ when the zeroth sample instant deviates from the uniform grid by $\epsilon_0 = -0.2T$. When the inter-sample distance is smaller than T, the magnitude of $G(t)$ is small. Whereas the interval with inter-sample distance larger than T has a large magnitude for $G(t)$.

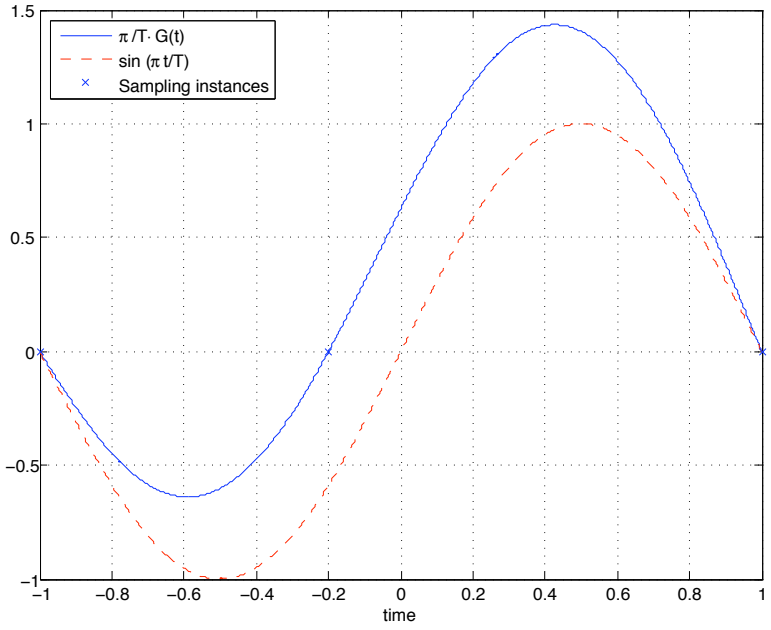

Figure 4-1: Plot of $G(t)$ (solid) when one sampling instant deviates from uniform grid by $\epsilon_0 = -0.2$, and sine function (dashed).

Another key characteristic of the Lagrange interpolation function, $l_n(t)$ is that it satisfies the interpolation property

$$l_n(t_k) = \begin{cases} 0, & n \neq k \\ 1, & n = k \end{cases}. \tag{4.9}$$

If the sampling instants are identical to the reconstruction time instants, this also implies the property of consistent resampling, i.e. resampling the reconstructed signal on the non-uniform grid $\{t_n\}$ yields the original samples $\{x(t_n)\}$. Representing the reconstruction and sampling processes by operator P, consistent sampling indicates that P is an idempotent operator, i.e. $P^2 = P$.

Equation (4.9) shows that the Lagrange interpolation function has zeros at all the sample locations except at the time instant where we evaluate the interpolation function, i.e. $t = t_n$. From Eqn. (4.1c), $G(t)$ is a product of factors involving all the sample instants, and thus $G(t)$ contributes to all the zeros of the Lagrange interpolation function. For sample instant $t_n|_{n=k}$, the factor $\frac{1}{t-t_k}$ in the Lagrange interpolation function contributes a pole that is cancelled by a corresponding zero in $G(t)$. The result of this pole-zero cancellation is

$$H_k(t_k) = \lim_{t \to t_k} \frac{G(t)}{t - t_k}. \tag{4.10}$$

Since the interpolating property of the Lagrange kernel states that $l_k(t_k) = 1$, the role of $G'(t)$ is to normalize Eqn. (4.10). As $G(t)$ is differentiable,

$$\begin{aligned} l_k(t_k) = \lim_{t \to t_k} \frac{G(t)}{(t - t_k)G'(t_k)} &= 1 \\ G'(t_k) &= \lim_{t \to t_k} \frac{G(t)}{t - t_k}. \end{aligned} \tag{4.11}$$

It is important to note that the maximum value of the Lagrange interpolation function need not occur at the sample instants t_n and it is not necessary that $\max_t(l_n(t)) = 1$. This is a property which has also been observed and described in [33].

The following list summarizes the characteristics of the Lagrange interpolation function:

1. G(t) is continuous at t_n and $G'(t_n) \neq 0$,

2. the zeros of $G(t)$ occur at the sampling instants t_n,

3. the magnitude of $\frac{\pi}{T}G(\bar{t})$, where $\bar{t} \in (t_n, t_{n+1})$, is greater than 1 when the inter-sample

distance is larger than T and is smaller than 1 when the inter-sample distance is smaller than T,

4. $G(t)$ accounts for the zeros in the interpolating property of $l_n(t)$,

5. $G'(t_n)$ is a normalizing factor that accounts for the required gain in the interpolating property, and

6. the maximum of the interpolating function does not have to occur at the sampling locations.

4.2 Framework for Approximations of the Lagrange Kernel

In this section, we formulate a representation for $G(t)$ based on the characteristics observed in Section 4.1. A special case of $G(t)$ occurs when the zeros are uniformly spaced at $t_n = nT$ and so

$$G(t) = \frac{T}{\pi} \sin\left(\frac{\pi}{T} t\right) \ . \tag{4.12}$$

In the case where the zeros are non-uniformly spaced at t_n, Eqn. (4.12) can be warped with a function $\beta(t)$ to relocate the uniformly spaced zeros so that $\sin(\frac{\pi}{T}\beta(t_n)) = 0$. We do not want to create additional zeros and a sufficient condition would require $\beta(t)$ to be strictly monotonically increasing, $\beta'(t) > 0$. This imposes the constraint of $\beta(t_n) = nT$ on the warping function.

We can relate $G(t)$ to the sine-type function by representing $G(t)$ as a modulated time-warped sine function

$$G(t) = s(t) \sin\left(\frac{\pi}{T}\beta(t)\right), \tag{4.13}$$

where $s(t)$ is a modulating function that represents the effects of the inter-sample distance on $G(t)$. The derivative of $G(t)$ is

$$G'(t) = s'(t) \sin\left(\frac{\pi}{T}\beta(t)\right) + \frac{\pi}{T} s(t)\beta'(t) \cos\left(\frac{\pi}{T}\beta(t)\right)$$

and at $t = t_n$,

$$G'(t_n) = \frac{\pi}{T} s(t_n)\beta'(t_n)(-1)^n. \tag{4.14}$$

Since $G(t)$ has simple roots at the instants t_n, $G'(t_n)$ is non-zero and so

$$\begin{aligned} |G'(t_n)| = \left|\frac{\pi}{T} s(t_n)\beta'(t_n)(-1)^n\right| &> 0 \\ |s(t_n)\beta'(t_n)| &> 0\,, \end{aligned}$$

where the constraint $\beta'(t) > 0$ implies that $|s(t_n)| > 0$. Furthermore, $G(t)$ is non-zero everywhere except at $\{t_n\}$ and so it is necessary that $s(t)$ is constrained by $0 < A \leq s(t) \leq B < \infty$, where A and B are positive constants.

A fixed $G(t)$ is not associated with a unique choice of $\{\beta(t),\, s(t)\}$. If $G(t)$ and $\beta(t)$ are fixed, then $s(t)$ is uniquely defined by

$$s(t) = \begin{cases} \frac{G(t)}{\sin\left(\frac{\pi}{T}\beta(t)\right)}, & t \neq t_n, \quad n \in \mathbb{Z} \\ \frac{T}{\pi}(-1)^n \frac{G'(t_n)}{\beta'(t_n)}, & t = t_n, \quad n \in \mathbb{Z}\,. \end{cases} \tag{4.15}$$

For the case when both $G(t)$ and $s(t)$ are fixed, there is a unique $\beta(t)$ such that

$$\beta(t) = \left(k - \frac{1}{2}\right)\frac{\pi}{T} + \frac{T}{\pi}\arcsin\left(\frac{G(t - (k-\frac{1}{2})\frac{\pi}{T})}{s(t - (k-\frac{1}{2})\frac{\pi}{T})}\right), \quad k \in \mathbb{Z}\,, \tag{4.16}$$

where $\beta(t)$ is defined only when $|s(t)| \geq |G(t)|$. This condition ensures that within each interval $t_n \leq t < t_{n+1}, \forall n \in \mathbb{Z}$, $G(t)$ can be warped from the range of values of $s(\beta^{-1}(t))\sin(\frac{\pi}{T}t)$.

The Lagrange interpolation function is alternatively represented as

$$\begin{aligned} l_n(t) = \frac{G(t)}{G'(t_n)(t-t_n)} &= \frac{s(t)\sin\left(\frac{\pi}{T}\beta(t)\right)}{\frac{\pi}{T}s(t_n)\beta'(t_n)(-1)^n(t-t_n)} \\ &= \frac{s(t)\sin\left(\frac{\pi}{T}(\beta(t)-nT)\right)}{s(t_n)\beta'(t_n)\frac{\pi}{T}(t-t_n)}, \end{aligned} \tag{4.17}$$

and so the reconstruction of a band-limited signal from its non-uniform samples is

$$\hat{x}(t) = \sum_{n=-\infty}^{\infty} x(t_n)\frac{s(t)\sin\left(\frac{\pi}{T}(\beta(t)-nT)\right)}{s(t_n)\beta'(t_n)\frac{\pi}{T}(t-t_n)}. \tag{4.18}$$

Fig. 4-2 shows an alternative representation of non-uniform sampling and reconstruction using the Lagrange kernel, where the reconstruction kernel is constructed by warping a sine function. It takes on a similar form as the system in Fig. 2-2, but with an additional pre-modulation by $1/s(t)\beta'(t)$ before the non-uniform sampling and reconstruction process and

post-modulation by $s(t)$ as the final stage.

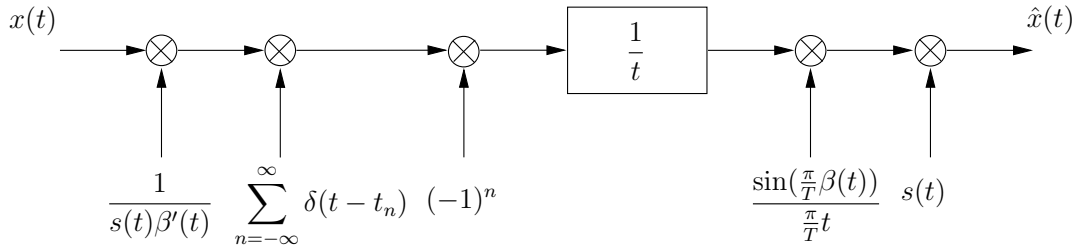

Figure 4-2: Representation of alternative Lagrange interpolation system.

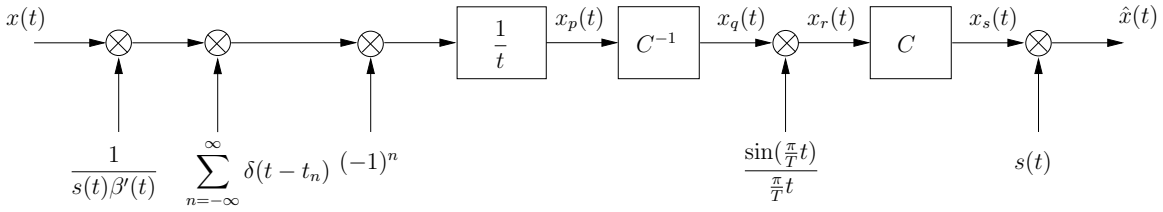

Figure 4-3: Equivalent non-uniform sampling and reconstruction using time-warping.

Another interpretation of Eqn. (4.18) is to warp the output of the Hilbert transformer instead of warping the sine function. The block diagram of this interpretation is shown in Fig. 4-3 and it is equivalent to the system in Fig. 4-2 up to and including the Hilbert transformer. The signal at the output of the Hilbert transformer is

$$x_p(t) = \sum_{n=-\infty}^{\infty} \frac{x(t_n)}{s(t_n)\beta'(t_n)} \frac{(-1)^n}{t - t_n} \,. \tag{4.19}$$

Passing $x_p(t)$ through the inverse warping operator C^{-1} with impulse function as given in Eqn. (3.7).

$$x_q(t) = x_p(\beta^{-1}(t)) = \sum_{n=-\infty}^{\infty} \frac{x(t_n)}{s(t_n)\beta'(t_n)} \frac{(-1)^n}{\beta^{-1}(t) - t_n} \,. \tag{4.20}$$

Modulating $x_q(t)$ with the sine function gives the input to the warping operator as

$$x_r(t) = \sum_{n=-\infty}^{\infty} x(t_n) \frac{\sin \frac{\pi}{T}(t - nT)}{s(t_n)\beta'(t_n)\frac{\pi}{T}(\beta^{-1}(t) - t_n)} \,. \tag{4.21}$$

The next step requires warping $x_r(t)$ by the operator C with impulse response defined by

Eqn. (3.5) to give

$$x_s(t) = x_r(\beta(t)) = \sum_{n=-\infty}^{\infty} x(t_n) \frac{\sin \frac{\pi}{T}(\beta(t) - nT)}{s(t_n)\beta'(t_n)\frac{\pi}{T}(t - t_n)} \,. \tag{4.22}$$

Lastly, $x_s(t)$ is modulated by $s(t)$ to obtain

$$\begin{aligned} \hat{x}(t) &= s(t)x_s(t) \\ &= \sum_{n=-\infty}^{\infty} x(t_n) \frac{s(t) \sin \frac{\pi}{T}(\gamma(t) - nT)}{s(t_n)\beta'(t_n)\frac{\pi}{T}(t - t_n)} \,. \end{aligned} \tag{4.23}$$

This alternative representation by warping the signals can be interpreted as performing the modulation with a sine function in a space spanned by warped sinc functions.

4.3 Approximation Methods

In this section, we approximate the Lagrange interpolation function using three different methods. Reconstruction by shifted sinc functions is presented using the framework of Eqn. (4.13). We then form approximations to $G(t)$ by constructing $s(t)$ and $\beta(t)$ as piecewise polynomials. Another approximation method involves approximating $G(t)$ with non-uniform splines, while maintaining the Lagrange kernel characteristics in the approximation.

4.3.1 Approximation using sinc function

Assume that the sampling instants $t_n = nT + \epsilon_n$, where ϵ_n are the deviations from the uniform grid. We define $G_n(t)$ as a sine function that is shifted by ϵ_n and so

$$G_n(t) = \frac{\sin(\frac{\pi}{T}(t - \epsilon_n))}{\pi/T}. \tag{4.24}$$

The derivative of Eqn. (4.24) is

$$G_n'(t) = \cos\left(\frac{\pi}{T}(t - \epsilon_n)\right) \tag{4.25}$$

which when evaluated at t_n, has the value $G'_n(t_n) = (-1)^n$. Let the scaled Hilbert transformer remain as $h(t) = 1/t$. This gives the approximation as

$$\begin{aligned} \hat{x}(t) &= \sum_{n=-\infty}^{\infty} x(t_n) \frac{G_n(t)}{(t-t_n)G'_n(t_n)} \\ &= \sum_{n=-\infty}^{\infty} x(t_n) \frac{\sin(\frac{\pi}{T}(t-t_n))}{\frac{\pi}{T}(t-t_n)} \end{aligned} \tag{4.26}$$

The sinc kernel $l_n(t) = \frac{\sin(\frac{\pi}{T}(t-t_n))}{\frac{\pi}{T}(t-t_n)}$ does not satisfy the interpolation property since $l_n(t_n) = 1$ while $l_n(t_k) \neq 0$ for $n \neq k$. Hence, for non-uniform sample instants, this approximation method causes inter-symbol interference and does not result in consistent sampling.

For the special case where the deviations from the uniform grid are equal and constant such that $\epsilon_n = \epsilon$, Eqn. (4.26) becomes

$$\hat{x}(t) = \sum_{n=-\infty}^{\infty} x(nT+\epsilon) \frac{\sin(\frac{\pi}{T}(t-nT-\epsilon))}{\frac{\pi}{T}(t-nT-\epsilon)} \tag{4.27}$$

and this perfectly reconstructs $x(t)$. Another way of forming an approximation is to assume that the samples lie on the uniform grid and through sinc interpolation,

$$\hat{x}(t) = \sum_{n=-\infty}^{\infty} x(t_n) \frac{\sin(\frac{\pi}{T}(t-nT))}{\frac{\pi}{T}(t-nT)}. \tag{4.28}$$

In this approximate reconstruction, the sinc reconstruction kernel satisfies the interpolation property on the uniform grid and there is no inter-symbol interference. However, Eqn. (4.28) does not fulfill the consistent resampling property, and the samples are not at the correct sample instants which leads to error in the reconstruction. This method can be used when the sample instants are unknown.

Figs. 4-4(a) and 4-4(b) respectively show the interpolation of the non-uniform samples using the shifted sinc approximation and the reconstruction using sinc interpolation while assuming the sample instants to be on the uniform grid.

The methods involving the sinc functions are unable to approximate the signal while satisfying the consistent resampling property. More accurate approximations to $G(t)$ can be obtained by constraining the approximations to satisfy the Lagrange interpolation function properties discussed in section 4.1.

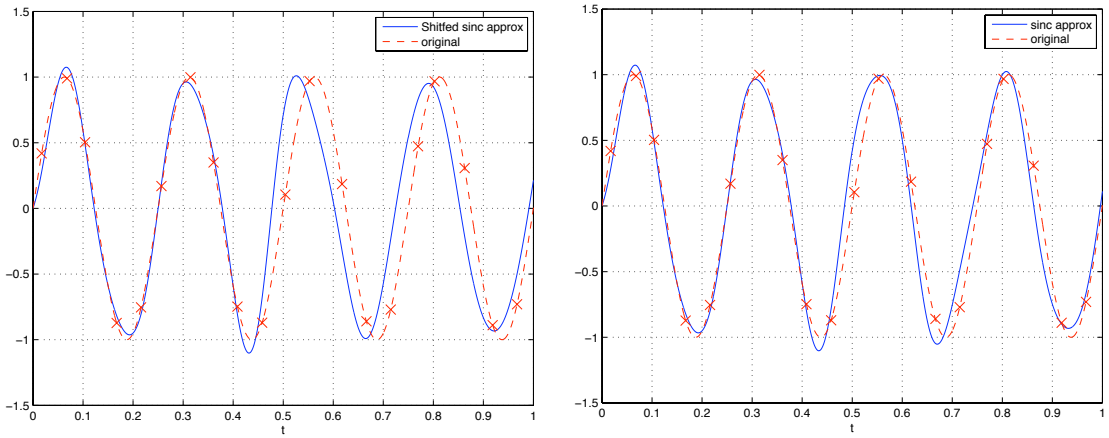

(a) (b)

Figure 4-4: Plots of approximation using (a) shifted sinc approximation and (b) sinc filter.

4.3.2 Approximation with piecewise sinusoids

Using Eqn. (4.13), $G(t)$ can be approximated by forming $\beta(t)$ and $s(t)$ as piecewise polynomial functions. In this subsection, we will approximate $G(t)$ as a piecewise sinusoidal function by forming $s(t)$ as a piecewise constant function and $\beta(t)$ as a piecewise linear function with non-equidistant constraint points at $\{t_n\}$ such that $\beta(t_n) = nT$. $\beta(t)$ can be expressed as

$$\beta(t) = \sum_{n=-\infty}^{\infty} \left[nT + \frac{T}{T_n}(t - t_n) \right] [u(t - t_n) - u(t - t_{n+1})] \tag{4.29}$$

where

$$u(t) = \begin{cases} 0, & t \leq 0 \\ 1, & t > 0 \end{cases}$$

and the interval of each piece is

$$T_n = |t_n - t_{n+1}|. \tag{4.30}$$

Substituting Eqn. (4.29) into Eqn. (4.13), $\hat{G}(t)$ can be expressed as

$$\hat{G}(t) = s(t) \sum_{n=-\infty}^{\infty} \sin\left(\frac{\pi}{T} \left(nT + \frac{T}{T_n}(t - t_n) \right) \right) (u(t - t_n) - u(t - t_{n+1})) \,. \tag{4.31}$$

Let $s(t)$ be a piecewise constant function with $s(t) = A_n > 0$, for $t_n \leq t < t_{n+1}$ and so $\hat{G}(t)$ is formulated a piecewise sinusoidal function such that

$$\hat{G}(t) = \sum_{n=-\infty}^{\infty} A_n \sin\left(\frac{\pi}{T}\left(nT + \frac{T}{T_n}(t - t_n)\right)\right)\left[u(t - t_n) - u(t - t_{n+1})\right] . \tag{4.32}$$

The amplitudes, A_n of the piecewise sinusoids are constrained to ensure that the derivatives of $\hat{G}(t)$ are continuous at the sample instants, t_n. This requires that

$$\begin{aligned}
\lim_{t \to t_n^-} \hat{G}(t) &= \lim_{t \to t_n^+} \hat{G}(t) \\
\lim_{t \to t_n^-} s_{n-1}(t)\frac{\pi}{T_{n-1}} \cos\left(\pi(n-1) + \frac{\pi}{T_{n-1}}(t - t_{n-1})\right) &= \lim_{t \to t_n^+} s_n(t)\frac{\pi}{T_n} \cos\left(\pi n + \frac{\pi}{T_n}(t - t_n)\right) \\
A_{n-1}\frac{\pi}{T_{n-1}} &= A_n\frac{\pi}{T_n} \\
A_n &= \frac{T_n}{T_{n-1}}A_{n-1}, \quad n \in \mathbb{Z} ,
\end{aligned} \tag{4.33}$$

which implies that A_n is proportional to the inter-sample distance T_n.

4.3.3 Approximation with non-uniform splines

One common approach to approximate reconstruction from non-uniform samples is to directly interpolate the samples with non-uniform splines [6]. However, our approach is to instead use non-uniform splines to approximate $G(t)$. In this formulation, we use B-splines for their smoothness as well as their finite support, which makes them computationally easy to implement.

$G(t)$ is approximated by creating a function $\tilde{G}(t)$ that behaves like Eqn. (4.13), i.e. constraining the zeros of $\tilde{G}(t)$ to be at the sampling instants t_n, which is analogous to approximating $\beta(t)$. This is implemented by placing an additional sequence of constraint points at the arithmetic mean of two sampling instants, and scaling the magnitude of the extra constraint points to be proportional to the inter-sampling distance. The series of constraint points of $\tilde{G}(t)$ at the sampling instants $t_i = \tau_{2i}$ are

$$\tilde{G}(\tau_{2i}) = 0, \quad i \in \mathbb{Z} \tag{4.34}$$

while the extra constraint points at instants $\tau_{2i+1} = \frac{t_i + t_{i+1}}{2}$ are given by

$$\tilde{G}(\tau_{2i+1}) = (-1)^i |t_{i+1-t_i}|^p, \quad i \in \mathbb{Z}, p \in \mathbb{R} \tag{4.35}$$

where p is a weighting factor that will be dependent on the degree of spline used, and this is analogous to forming $s(t)$.

For a given set of instants $\{\tau_0, \tau_1, \ldots, \tau_{N+1}\}$, a non-uniform B-spline of degree N is defined as given in [24].

$$B_N(t; \tau_0, \ldots, \tau_{N+1}) = \frac{(\tau_{N+1} - \tau_0)}{(-1)^{N+1}} \sum_{k=0}^{N+1} \frac{(t - \tau_k)^N u(t - \tau_k)}{D(\tau_k)} \tag{4.36}$$

where

$$D(\tau_k) = \prod_{\substack{l=0 \\ l \neq k}}^{N+1} (\tau_k - \tau_l) \ .$$

Since the sample instants are non-uniform, $B_N(t)$ is not shift-invariant. In addition, the degree N controls the smoothness of the approximation, and since $G(t)$ has to be at least continuous, this constrains the splines to be of degree $N \geq 2$. Using the N^{th} order B-splines given in Eqn. (4.36), the approximation to $G(t)$ is

$$\tilde{G}(t) = \sum_{i=-\infty}^{\infty} c_i B_N(t; \tau_i, \ldots, \tau_{i+N+1}) \tag{4.37}$$

where $\{c_i\}$ can be obtained from the constraint points $\{\tilde{G}(\tau_i)\}$ by solving a linear system of equations.

Fig. 4-5(a) shows the approximation of a warped sine function and 4-5(b) shows how the weighting factor p can achieve the effect of a modulated warped sine function.

From the approximation to $G(t)$ in Eqn. (4.37), we form the set of interpolating functions as

$$l_n(t) = \frac{\tilde{G}(t)}{\tilde{G}'(t_n)(t - t_n)}, \ \ n \in \mathbb{Z} \ . \tag{4.38}$$

The set of interpolation functions for the spline approximation method is shown in Fig. 4-6, where the interpolating kernels fulfill the interpolation property. It can also be observed that the maximum point of the interpolating kernels does not have to be at the sample instants t_n.

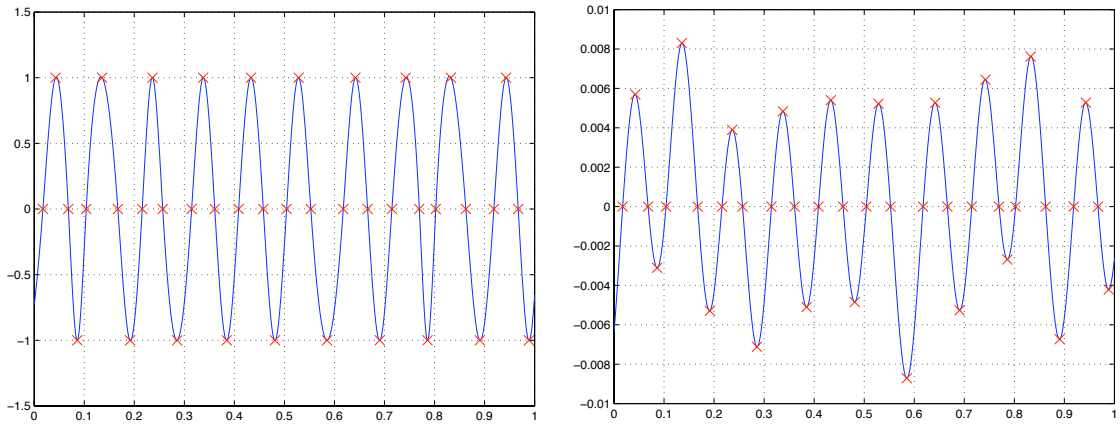

(a) (b)

Figure 4-5: (a) Cubic spline and (b) weighted cubic interpolation of sine-type function.

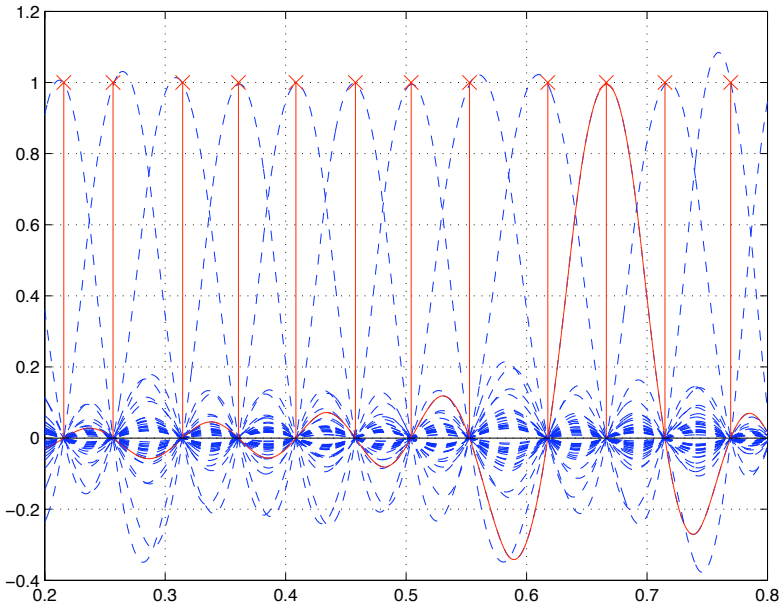

Figure 4-6: Interpolating property obtained by forming the interpolation kernels with non-uniform splines.

The importance of the weighting factor in obtaining a better approximation can also be shown by comparing Figs. 4-7(a) and 4-7(b), which show the interpolation results of approximating $G(t)$ with an unweighted cubic spline and a weighted cubic spline respectively. In both figures, the original sinusoidal signal of 4Hz, as shown by the dashed line, is sampled non-uniformly at $t_n = nT + \epsilon_n$, where $T = 0.05$s and ϵ_n is a sequence of independent and identically distributed (i.i.d.) uniform random variables with support of $[-0.25T, 0.25T]$s. In the weighted spline approximation, the value of $p = 1.735$ obtains the best approximation.

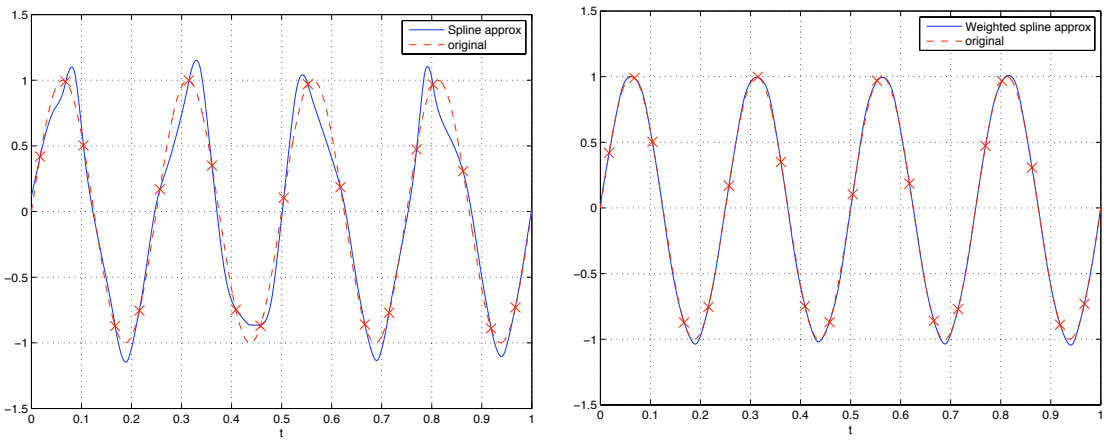

(a) (b)

Figure 4-7: Plot of approximate interpolation with (a) unweighted cubic spline approximation and (b) weighted cubic spline approximation

The amount of computations required to perform the N^{th} degree spline interpolation for $\tilde{G}(t)$ is on the same order as the computation required for the N^{th} degree direct spline interpolation of the nonuniform samples. This is because the constraint points accounting for the zeros of $G(t)$ do not add to the computational requirements, leaving the computation of $\tilde{G}(t)$ to depend only on the additional set of constraint points in Eqn. (4.35).

4.4 Numerical Experiments

In this section, we present the simulation results that illustrate the performance of the approaches for approximating $G(t)$. We specifically compare the performance of the methods using non-uniform cubic spline and piecewise sinusoid approximation of $G(t)$ with that of a direct cubic spline approximation of the signal. The optimal weighting factor for cubic

splines was found experimentally to be $p = 1.735$.

The first set of simulations was performed by sampling approximately band-limited white noise with support of $[-5, 5]$s. The signals were sampled non-uniformly with average sampling period of $T = 0.05$s and with the signal bandwidth varying from 0 to π/T rad/s. Let r be the bandwidth-sampling frequency ratio. The deviations of the sampling times from the uniform grid were a sequence of independent and identically distributed (i.i.d.) random variables drawn from a uniform distribution with support of $[-0.25T, 0.25T]$s. The reconstruction error was evaluated in the region of $[-1, 1]$s to mitigate the end effects. To evaluate the reconstruction performance, we compute the normalized mean squared error (MSE) of the output.

$$MSE = \frac{\int_1^{-1} |\hat{x}(t) - x(t)|^2 dt}{\int_1^{-1} |x(t)|^2 dt} \tag{4.39}$$

The average MSE was taken from 100 realizations of the reconstruction.

From Fig. 4-8, we see that the error for the direct spline interpolation increases faster than the reconstruction error of the two proposed methods involving the approximation of $G(t)$ as r increases. Though the proposed methods have a larger error when r is small, the spline approximation of $G(t)$ and the piecewise sinusoidal approximation of $G(t)$ perform better than direct spline approximation when $r > 0.3470$ and $r > 0.4653$ respectively. Specifically, the proposed methods become preferable for the case of sampling and reconstruction from non-uniform samples as the average sampling rate approaches the Nyquist rate.

An intuitive explanation of the simulation starts from the fact that $G(t)$ and the Lagrange interpolation functions are both band-limited functions. Approximation of $G(t)$ with piecewise functions maintains all the zeros. This translates to a sharp decay at π/T rad/s for the Fourier transform of $l_n(t)$. In contrast, the Fourier transform of the cardinal cubic spline function decays as $1/|\Omega|^4$ and so signal frequency components near π/T rad/s are attenuated. Therefore, the direct spline approximation tends to result in a good reconstruction for a low signal bandwidth relative to π/T rad/s, but does not work as well for signals with a larger bandwidth relative to π/T rad/s. Direct spline interpolation with higher degree splines will lead to better performance since the Fourier transform of the cardinal function will tend towards the frequency response of an ideal low-pass filter as the degree of the spline increases [2].

For small values of r, the proposed approximation methods have larger reconstruction errors due to oscillations arising from the inability to fulfill the partition of unity property

$$\sum_{n=-\infty}^{\infty} \frac{L(t)}{L'(t_n)(t-t_n)} = 1 \tag{4.40}$$

which is a necessary condition for reconstructing constant signals. Future work will consider approximations which account for this property.

In the second set of simulations, the amount of deviation of the sampling instant from the uniform grid is varied. In this case, the deviations of the sampling times from uniform were a sequence of i.i.d. random variables drawn from a uniform distribution with support that varied from 0s to $[-0.25T, 0.25T]$s. The signal bandwidth was maintained at 18π rad/s. Fig. 4-9 shows the MSE plots for the same methods of approximation as the previous simulation. The result shows that when the sampling rate is slightly greater than the Nyquist rate, the methods of approximating $G(t)$ have an improvement over direct spline interpolation for all deviation values.

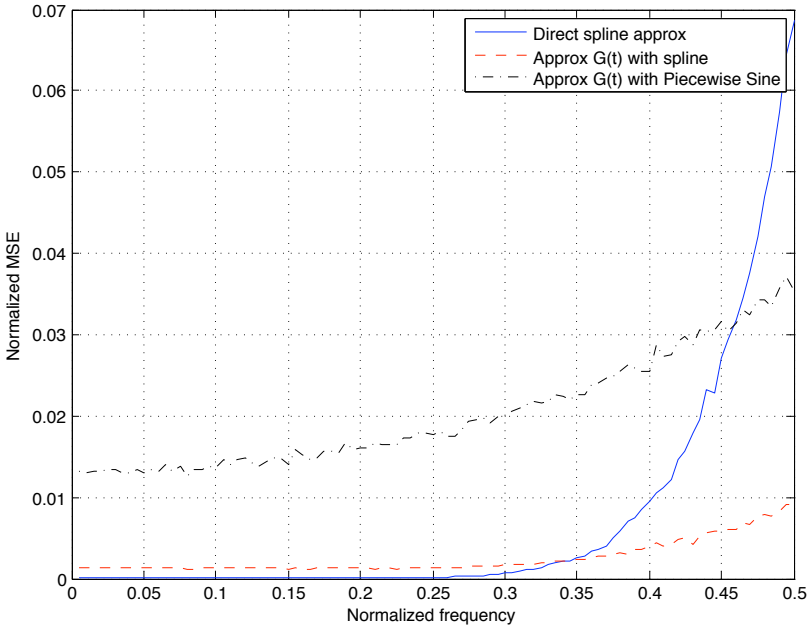

Figure 4-8: Reconstruction MSE by varying normalize frequency.

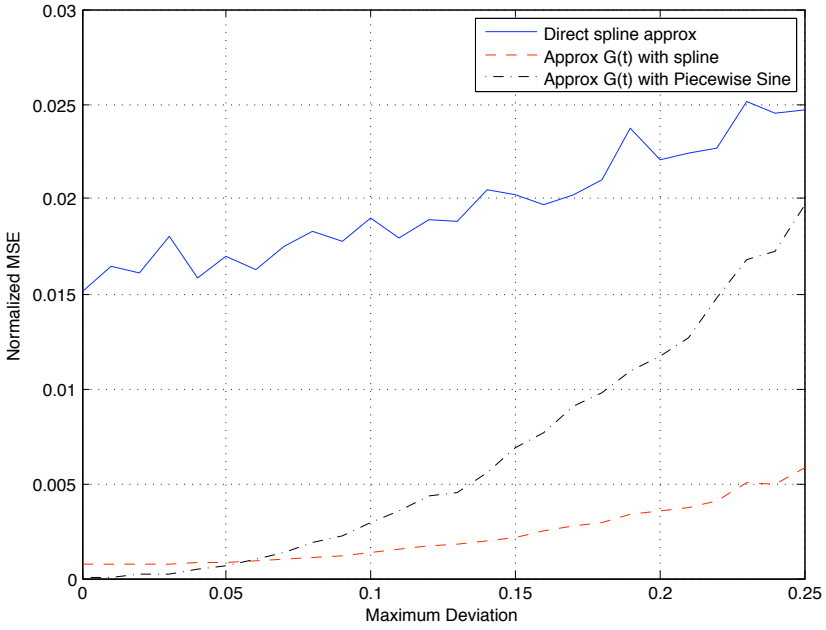

Figure 4-9: Reconstruction MSE by varying deviation from the uniform grid.

Chapter 5

Vector Space Representation and Iterative Reconstruction

In this chapter, we study the problem of non-uniform sampling using an abstract vector space representation of non-uniform sampling and reconstruction. This is based upon earlier work done by Dey [26] on abstract vector space representation of non-uniform sampling and aliasing. In the second part of the chapter, we perform signal reconstruction from non-uniform samples with an iterative algorithm studied by Gröchenig [11], Wiley [30] and Marvasti *et.* al. [20]. The algorithm is modified using a warped sinc function to obtain a faster rate of convergence.

5.1 Abstract Vector Space Representation of Non-uniform Sampling and Interpolation

In this section, we represent non-uniform sampling and interpolation with an abstract vector space formulation. We use this vector space perspective to analyze the effect of aliasing due to reconstruction from non-uniform samples.

Assume that the signals of interest belong to the space of finite energy signals, i.e. L_2 space. The L_2 space can be expressed as a direct-sum decomposition into a low-pass component and a high-pass component such that

$$L_2 = \mathcal{V} \oplus \mathcal{W} \tag{5.1}$$

where $\mathcal{V}$ is the space of signals band-limited to $(-\omega_0, \omega_0)$, and $\mathcal{W}$ is the space of signals that are band-limited to $(-\infty, -\omega_0] \cup [\omega_0, \infty)$. Let $x_{\mathcal{V}}(t) \in \mathcal{V}$ and $x_{\mathcal{W}}(t) \in \mathcal{W}$, with corresponding Fourier transforms of $X_{\mathcal{V}}(\omega)$ and $X_{\mathcal{W}}(\omega)$ respectively. The Fourier transforms $X_{\mathcal{V}}(\omega)$ and $X_{\mathcal{W}}(\omega)$ are orthogonal under the inner product

$$\langle X_{\mathcal{V}}(\omega), X_{\mathcal{W}}(\omega) \rangle = \int_{-\infty}^{\infty} X_{\mathcal{V}}(\omega) X_{\mathcal{W}}^*(\omega)\, d\omega \tag{5.2}$$

which by Parseval's theorem

$$\begin{aligned} \int_{-\infty}^{\infty} X_{\mathcal{V}}(\omega) X_{\mathcal{W}}^*(\omega)\, d\omega &= \int_{-\infty}^{\infty} x_{\mathcal{V}}(t) x_{\mathcal{W}}^*(t)\, dt \\ &= \langle x_{\mathcal{V}}(t), x_{\mathcal{W}}(t) \rangle \ . \end{aligned} \tag{5.3}$$

This implies that $x_{\mathcal{V}}(t)$ and $x_{\mathcal{W}}(t)$ are orthogonal under the inner product in Eqn. (5.3) and so $\mathcal{V}$ is orthogonal to $\mathcal{W}$.

Let the linear operator $f(\cdot)$ represent the composition of sampling at time instants t_n and reconstruction with the Lagrange kernel $l_n(t)$, where the domain of $f(\cdot)$ is L_2. Assume that the sampling density is ω_0/π and the sample instants t_n satisfy the constraint given in Eqn. (2.18). These assumptions are sufficient for the Lagrange kernel output to be a function with Fourier transform band-limited to $(-\omega_0, \omega_0)$, and so the operator $f(\cdot)$ has range, $\mathcal{R}(f) = \mathcal{V}$. From the non-uniform sampling theorem in Eqns. (2.18) - (2.19), a function $x_{\mathcal{V}}(t) \in \mathcal{V}$ sampled at t_n will be perfectly reconstructed through Lagrange interpolation. This implies that $f(x_{\mathcal{V}}(t)) = x_{\mathcal{V}}(t)$. The Lagrange kernel, $l_n(t)$ fulfills the interpolation property, which is a sufficient condition for the operator $f(\cdot)$ to possess the consistent re-sampling property for any $x(t) \in L_2$,

$$f(f(x(t))) = f(x(t)) \ . \tag{5.4}$$

$\mathcal{N}(f)$ is the null space of $f(\cdot)$ and it is the space that contains functions in L_2 which have zeros at all the time instants t_n. The interpolation property of $l_n(t)$ guarantees that every function in $\mathcal{N}(f)$ has zeros at all the time instants t_n. It can also be shown that the only vector that lives in both $\mathcal{V}$ and $\mathcal{N}(f)$ is the zero vector. A different direct-sum decomposition

of L_2 is induced by $f(\cdot)$ such that

$$L_2 = \mathcal{V} \oplus \mathcal{N}(f) \; . \tag{5.5}$$

The range space $\mathcal{R}(f) = \mathcal{V}$ and the null-space $\mathcal{N}(f)$ are not necessarily orthogonal for any sampling grid $\{t_n\}$.

The consistent re-sampling property in Eqn. (5.4) implies that $f(\cdot)$ is a projection operator, and since $\mathcal{V}$ is not orthogonal to $\mathcal{N}(f)$ for the case of non-uniform sampling, $f(\cdot)$ is an oblique projection onto the space $\mathcal{V}$ along the direction of $\mathcal{N}(f)$. Assume that a signal $x(t)$ in L_2 is composed of $x_{\mathcal{V}}(t) \in \mathcal{V}$ and $x_{\mathcal{W}}(t) \in \mathcal{W}$,

$$x(t) = x_{\mathcal{V}}(t) + x_{\mathcal{W}}(t) \; . \tag{5.6}$$

The effect of the oblique projection operator on $x(t)$ is

$$\begin{aligned} f(x(t)) &= f(x_{\mathcal{V}}(t) + x_{\mathcal{W}}(t)) \\ &= x_{\mathcal{V}}(t) + f(x_{\mathcal{W}}(t)) \; . \end{aligned} \tag{5.7}$$

Since $f(x(t)) \in \mathcal{V}$, the aliasing error in the subspace $\mathcal{V}$ induced by operator $f(\cdot)$ is given as an oblique projection of signals in the out-of-band space $\mathcal{W}$ onto the in-band space $\mathcal{V}$, where the aliased component is $f(x_{\mathcal{W}}(t))$. The above discussion shows that reconstruction from non-uniform samples of a non-bandlimited signal results in a band-limited reconstruction.

5.1.1 Reconstruction of non-uniform samples from out-of-band signals

The preceding abstract vector space description is used to show the effects of aliasing from non-uniform sampling and reconstruction using Lagrange interpolation. We specifically consider the case where the signal $x(t) = w(t)$ has a Fourier transform that is only non-zero in the frequency interval $(\omega_0, 3\omega_0)$. Uniform sampling of the signal is equivalent to a periodic replication of the signal spectrum in the frequency domain, and the aliased version that lies in $(-\omega_0, \omega_0)$ also takes on the same spectral shape as the signal spectrum in $(\omega_0, 3\omega_0)$. However, this is not necessarily true for non-uniform sampling.

In this part, we find the resultant aliased in-band signal when $w(t)$ is non-uniformly sampled and reconstructed using Lagrange interpolation. Alternatively, the aliasing problem

can be posed as finding an in-band signal $\tilde{v}(t) \in \mathcal{V}$ operated by $f(\cdot)$ such that

$$\tilde{v}(t) = f(\tilde{v}(t)) = f(w(t)) \; . \tag{5.8}$$

This means that we want to find the in-band signal $\tilde{v}(t)$ that is the projection through $f(\cdot)$ of $w(t)$ onto the space $\mathcal{V}$. Let $b(t) \in \mathcal{V}$ be the baseband modulated version of $w(t)$, where

$$w(t) = b(t)e^{j\frac{2\pi}{T}t} \; . \tag{5.9}$$

Non-uniform sampling of $w(t)$ at time instants $t_n = nT + \epsilon_n$, followed by Lagrange interpolation of the sample sequence is

$$\begin{aligned} f(w(t)) &= \sum_{n=-\infty}^{\infty} w(t_n) \frac{G(t)}{G'(t_n)(t-t_n)} \\ &= \sum_{n=-\infty}^{\infty} b(t_n) e^{j\frac{2\pi}{T}t_n} \frac{G(t)}{G'(t_n)(t-t_n)} \\ &= \sum_{n=-\infty}^{\infty} b(t_n) e^{j\frac{2\pi}{T}(nT+\epsilon_n)} \frac{G(t)}{G'(t_n)(t-t_n)} \\ &= \sum_{n=-\infty}^{\infty} b(t_n) e^{j\frac{2\pi}{T}\epsilon_n} \frac{G(t)}{G'(t_n)(t-t_n)} \; . \end{aligned} \tag{5.10}$$

Non-uniform sampling $\tilde{v}(t)$ at $\{t_n\}_{n\in\mathbb{Z}}$, followed by Lagrange interpolation is expressed as

$$f(\tilde{v}(t)) = \sum_{n=-\infty}^{\infty} \tilde{v}(t_n) \frac{G(t)}{G'(t_n)(t-t_n)}, \tag{5.11}$$

and from Eqn. (5.8),

$$\begin{aligned} f(w(t)) &= f(\tilde{v}(t)) \\ \sum_{n=-\infty}^{\infty} b(t_n) e^{j\frac{2\pi}{T}\epsilon_n} \frac{G(t)}{G'(t_n)(t-t_n)} &= \sum_{n=-\infty}^{\infty} \tilde{v}(t_n) \frac{G(t)}{G'(t_n)(t-t_n)} \; . \end{aligned} \tag{5.12}$$

Comparing both sides of Eqn. (5.12), the in-band signal $\tilde{v}(t)$, obtained from the oblique projection of $w(t)$ onto $\mathcal{V}$, has its sample values at t_n as

$$\tilde{v}(t_n) = b(t_n)e^{j\frac{2\pi}{T}\epsilon_n} \; . \tag{5.13}$$

In Eqn. (3.16), we formulated a delay modulation function $\alpha(t)$ with $\alpha(t_n) = \epsilon_n$ and so Eqn. (5.13) can be expressed as

$$\tilde{v}(t_n) = b(t_n)e^{j\frac{2\pi}{T}\alpha(t_n)} . \tag{5.14}$$

From the above result, the alias of $x_{\mathcal{W}}(t)$ under the operator $f(\cdot)$ can be approximated as its base-band version $b(t)$ modulated by $e^{j\frac{2\pi}{T}\alpha(t)}$, where

$$f(w(t)) \approx b(t)e^{j\frac{2\pi}{T}\alpha(t)} . \tag{5.15}$$

Modulation of the base-band version of $w(t)$ by a warped cosine function indicates that the aliased signal can be interpreted as a smearing of the frequency spectrum of $b(t)$. In the special case of uniform sampling, where $t_n = nT$ and $\epsilon_n = 0$, the projection of $w(t)$ by the operator $f(\cdot)$ gives $f(w(t)) = b(t)$, and this is equivalent to $\alpha(t) = 0$.

5.1.2 Warped sinc kernels as projections in vector space

Building on the idea that non-uniform sampling followed by Lagrange interpolation is an oblique projection of a signal onto the band-limited subspace, the approximate reconstruction methods can be examined to determine if they are equivalent to projections onto approximation spaces. Obtaining reconstruction methods which are projection operators is important because this allows consistent resampling to be achieved. A projection, P is a linear transformation that is idempotent, i.e. $P^2 = P$. This means that a projection operator is an operator which gives a consistent reconstruction of a function x that lies in any arbitrary Hilbert space. We observe that the approximate reconstruction by uniform sinc interpolation of non-uniform samples, which is defined by

$$\hat{x}(t) = \sum_{n=-\infty}^{\infty} x(t_n)\frac{\sin\frac{\pi}{T}(t-nT)}{\frac{\pi}{T}(t-nT)}, \tag{5.16}$$

is not a projection as it does not fulfill the consistent re-sampling property. However, Eqn. (5.16) can be modified to fulfill the consistent re-sampling property through time-warping the sinc kernel. The warped sinc reconstruction formula

$$\hat{x}(t) = \sum_{n=-\infty}^{\infty} x(t_n)\frac{\sin\frac{\pi}{T}(\beta(t)-nT)}{\frac{\pi}{T}(\beta(t)-nT)} \tag{5.17}$$

as presented in [5], [22] and [36], is a projection onto the subspace $\mathcal{V}_\beta$, i.e. the space spanned by low-pass filters with time-varying "bandwidths". We let the linear operator $g(\cdot)$ represent the process of non-uniform sampling at t_n and reconstruction with warped sinc functions. The corresponding range space is $\mathcal{R}(g) = \mathcal{V}_\beta$ and the null space consists of functions in L_2 that are zero at time instants t_n. Therefore, the null space of $g(\cdot)$ is $\mathcal{N}(g) = \mathcal{N}(f)$.

An illustration of the range spaces and null spaces of $f(\cdot)$ and $g(\cdot)$ is shown in Fig. 5-1.

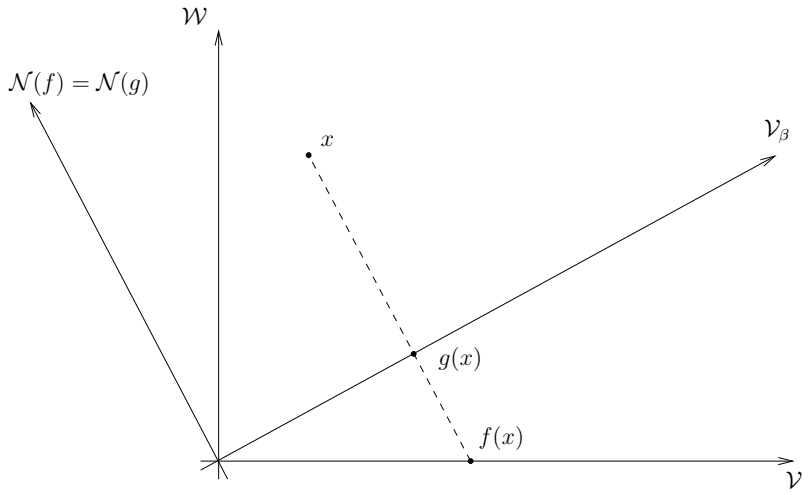

Figure 5-1: Projection onto band-limited subspace and subspace spanned by low-pass filters with time-varying "bandwidth".

The warping function $\beta(t)$ maps the subspace $\mathcal{V}$ to the subspace $\mathcal{V}_\beta$. The distance between these two spaces can be measured using the error resulting from the oblique projection by the operator $g(\cdot)$ of a signal in $\mathcal{V}$ onto $\mathcal{V}_\beta$. Assume that the original signal $x(t) = v(t) \in \mathcal{V}$. Using the operator $g(\cdot)$, the oblique projection of $x(t)$ onto the subspace $\mathcal{V}_\beta$ is given by Eqn. (5.17). The reconstruction error is

$$e_g(t) = x(t) - \hat{x}(t) \; . \tag{5.18}$$

We constrain the warping function $\beta(t)$ to be invertible and assume that there exist an m such that $0 < m \leq \beta'(t)$. The inverse warping function $\beta^{-1}(t)$ can be expressed as $\beta^{-1}(t) = t + \epsilon(t)$, where we constrain the delay modulation function $\epsilon(t)$ to satisfy $\epsilon(nT) = \epsilon_n$. Assume that $\epsilon(t)$ is a finite-energy function whose Fourier transform $E(\omega)$ is band-limited to $\frac{2\pi}{T}$ and let $\zeta = \max_\omega |E(\omega)|$. We also assume that $x(t)$ has a Fourier transform $X(\omega)$

with $\xi = \max_\omega |X(\omega)|$. By reformulating the error analysis in [36], it can be shown that the reconstruction error is bounded by

$$|e_g(t)| \leq \sqrt{2}\frac{4\pi}{T}\xi\zeta \cdot e^{\frac{2\pi\zeta}{T}} \tag{5.19}$$

and the energy of the reconstruction error is bounded by

$$\|e_g(t)\|_2^2 \leq \frac{3T\xi^2}{2m} \cdot e^{\frac{4\pi}{T}\zeta} \cdot \left(e^{\frac{2\pi\zeta}{T}} - 1\right)^2 , \tag{5.20}$$

which is dependent on the sampling period, T and the magnitude of the Fourier transform of $\epsilon(t)$. Eqn. (5.20) shows that the bound on the total error energy tends to zero as $\zeta \to 0$ and $2\pi/T \to 0$. This implies that as the magnitude and bandwidth of the Fourier transform of $\epsilon(t)$ becomes smaller, $\beta^{-1}(t) \to t$ and so $\beta(t)$ also tends to t, effectively bringing the space $\mathcal{V}_\beta$ "closer" to the subspace $\mathcal{V}$. The scope of this thesis does not consider how to select an optimal $\epsilon(t)$ and this is left for consideration in future work.

5.2 Iterative Reconstruction

This section considers an iterative method for reconstructing band-limited signals from non-uniform samples. The iterative reconstruction method is based on an algorithm used in [9], [10] and [11], which is a variant of the alternating projections algorithm [31]. It involves a sequence of projections onto some convex sets to obtain approximations that converge to the original signal. In this section, the convex sets are specifically chosen to be the in-band subspace $\mathcal{V}$ and the approximation subspace $\mathcal{V}_\beta$ spanned by warped sinc functions. These subspaces are linear and are therefore convex.

The methods in [11] involve the use of approximation subspace spanned by piecewise constant and piecewise linear functions. Since the original signal belongs to $\mathcal{V}$, the projection from $\mathcal{V}$ onto the space spanned by piecewise polynomial functions in general has a larger error in the projection as compared to $\mathcal{V}_\beta$, which leads to a long convergence time. The subspace, $\mathcal{V}_\beta$, spanned by warped sinc functions is in some sense closer to $\mathcal{V}$ and so leads to a faster convergence rate.

In this section, we formulate the iterative algorithm using warped sinc functions. The first subsection describes the iterative reconstruction algorithm using an abstract vector

space illustration. In the second subsection, we follow the derivation of the convergence rate in [11] to show that approximate reconstruction by projecting on the space spanned by warped sinc functions leads to a faster convergence rate.

5.2.1 Iterative reconstruction algorithm

The formulation of the iterative reconstruction algorithm used in this section was introduced by Gröchenig [11]. Let $\mathcal{Q}$ represent the operation of sampling $x(t) \in \mathcal{V}$ at instants t_n followed by reconstruction using Eqn. (5.17) to obtain $\hat{x}(t) \in \mathcal{V}_\beta$. This is equivalent to an oblique projection of $x(t)$ onto $\mathcal{V}_\beta$ along the null space of $\mathcal{Q}$,

$$\begin{aligned} \hat{x}(t) &= \mathcal{Q}x(t) \\ &= \sum_{n=-\infty}^{\infty} x(t_n) \frac{\sin \frac{\pi}{T}(\beta(t) - nT)}{\frac{\pi}{T}(\beta(t) - nT)} \end{aligned} \tag{5.21}$$

where $\beta(t)$ is an invertible warping function satisfying the constraint $\beta(t_n) = nT,\ \forall n \in \mathbb{Z}$. This constraint is sufficient for Eqn. (5.21) to satisfy the consistent re-sampling property, which gives

$$\hat{x}(t_n) = x(t_n), \quad \forall n \in \mathbb{Z}. \tag{5.22}$$

Let the operator $\mathcal{P}$ represent the filtering of $\hat{x}(t)$ with an ideal low-pass filter to obtain $\tilde{x}(t) \in \mathcal{V}$, which is an orthogonal projection of $\hat{x}(t)$ onto $\mathcal{V}$. Let the combination of the above two operations be represented by operator $\mathcal{S} = \mathcal{P}\mathcal{Q}$.

Assume that operator $\mathcal{S}$ satisfies $\|I - \mathcal{S}\|_2 < 1$, which is a sufficient condition guaranteeing the convergence of the algorithm [11]. The inverse of the operator is

$$\mathcal{S}^{-1} = \sum_{k=0}^{\infty} (I - \mathcal{S})^k, \tag{5.23}$$

where I is the identity operator. The reconstructed signal can thus be expressed as

$$\begin{aligned} x(t) &= \mathcal{S}^{-1}\mathcal{S}x(t) = \sum_{k=0}^{\infty} (I - \mathcal{S})^k \mathcal{S}x(t) \\ &= \mathcal{S}x(t) + (I - \mathcal{S})\mathcal{S}x(t) + (I - \mathcal{S})^2\mathcal{S}x(t) + (I - \mathcal{S})^3\mathcal{S}x(t) + \dots \\ &= \mathcal{S}x(t) + (I - \mathcal{S})\mathcal{S}x(t) + (I - \mathcal{S})[(I - \mathcal{S})\mathcal{S}x(t)] \\ &\quad + (I - \mathcal{S})[(I - \mathcal{S})^2\mathcal{S}x(t)] + \dots \end{aligned} \tag{5.24}$$

Let the zeroth approximation be

$$x_0(t) = 0 \tag{5.25}$$

and from Eqn. (5.24), the $(k+1)^{\text{th}}$ approximation of $x(t)$ can be expressed as

$$\begin{aligned} x_{k+1}(t) &= \mathcal{S}x(t) + (I - \mathcal{S})x_k(t) \\ &= [\mathcal{S}x(t) - \mathcal{S}x_k(t)] + x_k(t) \\ &= \mathcal{P}\mathcal{Q}[x(t) - x_k(t)] + x_k(t) \end{aligned} \tag{5.26}$$

such that

$$x(t) = \lim_{k\to\infty} x_k(t) \; . \tag{5.27}$$

This algorithm can be illustrated using the abstract vector space representation shown in Fig. 5-2. The numbers in Fig. 5-2 represent the steps of the algorithm described below. For steps 3 and 4, the figure illustrates the case when $k = 1$.

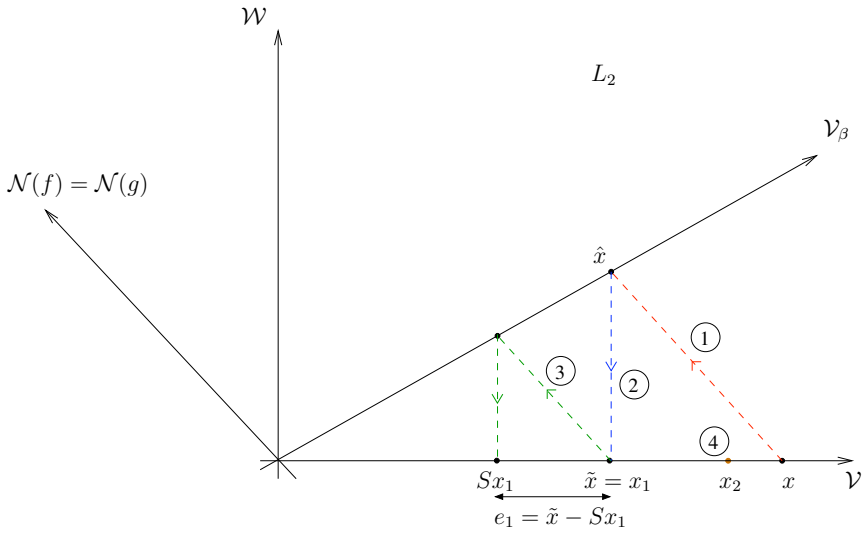

Figure 5-2: Illustration of iterative reconstruction algorithm.

Initialize index $k = 0$ and $x_0(t) = 0$.

1. Sample $x(t)$ at t_n and reconstruct using the warped sinc kernel in Eqn. (5.21) to obtain $\hat{x}(t)$, where this operation is represented by operator $\mathcal{Q}$.
2. Filter $\hat{x}(t)$ with an ideal low-pass filter to obtain $\tilde{x}(t)$, and let this operation be denoted by $\mathcal{P}$.

3. Let $\mathcal{S} = \mathcal{P}\mathcal{Q}$ and so $\tilde{x}(t) = \mathcal{S}x(t)$. Similarly, let $\mathcal{S}$ operate on $x_k(t)$.

4. Let $e_k(t)$ be the k^{th} approximation error between $\mathcal{S}x_k(t)$ and $\tilde{x}(t)$ so that

$$e_k(t) = \mathcal{S}x(t) - \mathcal{S}x_k(t). \tag{5.28}$$

Add the error $e_k(t)$ to $x_k(t)$ to obtain the $(k+1)^{\text{th}}$ approximation

$$x_{k+1}(t) = x_k(t) + e_k(t). \tag{5.29}$$

5. Let $k = k + 1$ and repeat steps 3 and 4.

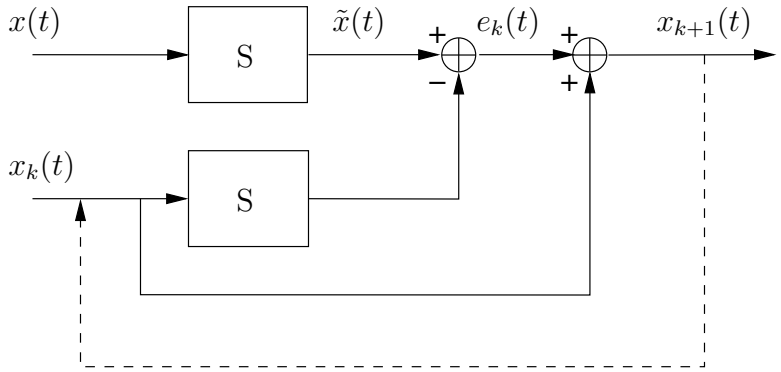

Figure 5-3: Block diagram of iterative reconstruction.

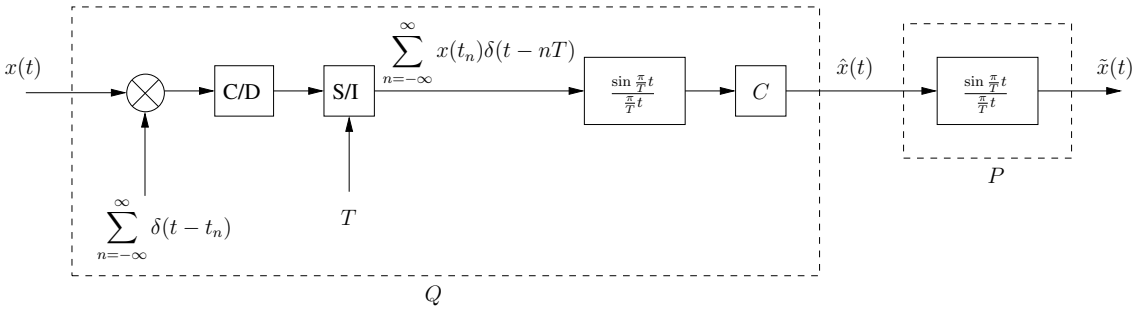

Figure 5-4: Block diagram of $\mathcal{S}$ operator.

The block diagram representation of the algorithm is shown in Fig. 5-3, where the detailed description of operator $\mathcal{S}$ is shown in the block diagram of Fig. 5-4. In this case,

we represent operator $\mathcal{Q}$ with the warped sinc interpolator. The dotted arrow in Fig. 5-3 indicates the update of $x_k(t)$ by $x_{k+1}(t)$.

5.2.2 Convergence of iterative algorithm

As shown in [11], the error between the original signal, $x(t) \in \mathcal{V}$ and the k^{th} approximate reconstuction, $x_k(t) \in \mathcal{V}$ can be bounded by

$$\|x - x_k\| \leq \|I - \mathcal{S}\|^{k+1} \frac{1 + \|I - \mathcal{S}\|}{1 - \|I - \mathcal{S}\|} \|x\| \ . \tag{5.30}$$

Since $\|I - \mathcal{S}\| < 1$, the term $\|I - \mathcal{S}\|^{k+1}$ in Eqn. (5.30) tends to zero as k tends to infinity. This shows that

$$\lim_{k \to \infty} \|x - x_k\| = 0 \tag{5.31}$$

and so the iterative algorithm obtains an approximation that converges to the original signal.

In the next part, we show that choosing the operator $\mathcal{Q}$ to project on the space spanned by warped sinc functions leads to a faster convergence rate than projecting onto the space spanned by piecewise linear functions. We use the method in [11] to estimate the error of non-uniform sampling and reconstructing $x(t)$ as $\|x - \mathcal{S}x\|$. Since $x(t) \in \mathcal{V}$, we get the identity $x = \mathcal{P}x$, and

$$\begin{aligned} \|x - \mathcal{S}x\|^2 &= \|\mathcal{P}x - \mathcal{P}\mathcal{Q}x\|^2 \\ &\leq \|x - \mathcal{Q}x\|^2 = \|x - \hat{x}\|^2 \\ &= \int_{-\infty}^{\infty} |x(t) - \hat{x}(t)|^2 dt \ . \end{aligned} \tag{5.32}$$

Let $\chi_n(t)$ be rectangular functions with support $[t_n, t_{n+1})$ such that the set of functions $\{\chi_n(t)\}$ form a partition of unity

$$\sum_{n=-\infty}^{\infty} \chi_n(t) = 1 \ , \tag{5.33}$$

and so we can express Eqn. (5.32) as

$$\int_{-\infty}^{\infty} |x(t) - \hat{x}(t)|^2 \sum_{n=-\infty}^{\infty} \chi_n(t) dt = \sum_{n=-\infty}^{\infty} \int_{t_n}^{t_{n+1}} |x(t) - \hat{x}(t)|^2 dt \; . \tag{5.34}$$

For each interval $[t_n, t_{n+1})$, there is a scaling function $\theta_n(t)$ such that

$$\theta_n(t) x(t) = x(t) - \hat{x}(t) \tag{5.35}$$

where the consistent re-sampling property of Eqn. (5.22) indicates that $\theta_n(t_n)x(t_n) = \theta_n(t_{n+1})x(t_{n+1}) = 0$.

Wirtinger's inequality states that if h, $h'' \in L^2(a, b)$ and $h(a) = h(b) = 0$, then

$$\int_a^b |h(t)|^2 dt \leq \left(\frac{b-a}{\pi}\right)^4 \int_a^b |h''(t)|^2 dt \; . \tag{5.36}$$

Using Wirtinger's inequality,

$$\begin{aligned}
& \sum_{n=-\infty}^{\infty} \int_{t_n}^{t_{n+1}} |\theta_n(t) x(t)|^2 dt \\
\leq \; & \sum_{n=-\infty}^{\infty} \left(\frac{t_{n+1} - t_n}{\pi}\right)^4 \int_{t_n}^{t_{n+1}} |\theta_n''(t) x(t) + 2\theta_n'(t) x'(t) + \theta_n(t) x''(t)|^2 dt \\
\leq \; & \sum_{n=-\infty}^{\infty} \left(\frac{t_{n+1} - t_n}{\pi}\right)^4 \left[\int_{t_n}^{t_{n+1}} |\theta_n''(t) x(t)|^2 dt + \int_{t_n}^{t_{n+1}} |2\theta_n'(t) x'(t)|^2 dt + \int_{t_n}^{t_{n+1}} |\theta_n(t) x''(t)|^2 dt\right] \\
\leq \; & \sum_{n=-\infty}^{\infty} \left(\frac{t_{n+1} - t_n}{\pi}\right)^4 \int_{t_n}^{t_{n+1}} |\theta_n(t) x''(t)|^2 dt \; .
\end{aligned} \tag{5.37}$$

If there exists a non-negative constant A such that

$$A = \max_n \int_{t_n}^{t_{n+1}} |\theta_n(t)|^2 dt \; , \tag{5.38}$$

and a non-negative constant δ such that $\delta = \max_n |t_{n+1} - t_n|$, then by Cauchy-Schwarz

inequality,

$$\begin{aligned}\sum_{n=-\infty}^{\infty}\left(\frac{t_{n+1}-t_n}{\pi}\right)^4\int_{t_n}^{t_{n+1}}|\theta_n(t)x''(t)|^2dt &\leq \sum_{n=-\infty}^{\infty}\left(\frac{\delta}{\pi}\right)^4\left(\int_{t_n}^{t_{n+1}}|\theta_n(t)|^2dt\int_{t_n}^{t_{n+1}}|x''(t)|^2dt\right)\\ &\leq A\left(\frac{\delta}{\pi}\right)^4\sum_{n=-\infty}^{\infty}\int_{t_n}^{t_{n+1}}|x''(t)|^2dt\\ &= A\left(\frac{\delta}{\pi}\right)^4\left\|x''(t)\right\|^2 \qquad (5.39)\end{aligned}$$

Bernstein's inequality states that if $h \in PW_{\omega_0}$, then $h' \in PW_{\omega_0}$ and

$$\left\|h'\right\| \leq \omega_0 \left\|h\right\| . \qquad (5.40)$$

We can obtain a further bound in Eqn. (5.39) by using Bernstein's inequality,

$$A\left(\frac{\delta}{\pi}\right)^4\left\|x''(t)\right\|^2 \leq A\left(\frac{\delta}{\pi}\right)^4{\omega_0}^2\left\|x'(t)\right\|^2 \leq A\left(\frac{\delta\omega_0}{\pi}\right)^4\left\|x(t)\right\|^2 . \qquad (5.41)$$

Therefore,

$$\left\|x(t)-\mathcal{S}x(t)\right\|^2 \leq A\left(\frac{\delta\omega_0}{\pi}\right)^4\left\|x(t)\right\|^2 \qquad (5.42)$$

and

$$\left\|I-\mathcal{S}\right\| \leq \sqrt{A}\left(\frac{\delta\omega_0}{\pi}\right)^2 . \qquad (5.43)$$

From Eqn. (5.30), the error between the original signal and the reconstruction from the k^{th} iteration is bounded by

$$\left\|x-x_k\right\| \leq \left(\sqrt{A}\left(\frac{\delta\omega_0}{\pi}\right)^2\right)^{(k+1)}\frac{\pi^2+\sqrt{A}(\delta\omega_0)^2}{\pi^2-\sqrt{A}(\delta\omega_0)^2}\left\|x\right\| . \qquad (5.44)$$

In comparison, the convergence rate obtained by piecewise linear approximation is given in [11] as Eqn. (5.43) with $A = 1$. If $\max_n|\theta_n(t)| < 1/\sqrt{\delta}$, this is a sufficient condition for $A < 1$, and the convergence rate using the warp sinc functions is faster than that for the piecewise linear approximation. Future work can be done to obtain a better bound on the convergence rate.

A simple simulation of the iterative algorithm is shown in Fig. 5-5 by comparing operator $\mathcal{Q}$ as a warped sinc interpolation, and with operator $\mathcal{Q}$ as a linear interpolation. The

simulation was performed by sampling approximately band-limited white noise with support of $[-5, 5]$s. The signals were sampled non-uniformly with average sampling period, $T = 0.05$s with the signal bandwidth varying from 0 to π/T. The deviations of the sampling times from the uniform grid were a sequence of independent and identically distributed (i.i.d.) random variables drawn from a uniform distribution with support of $[-0.2T, 0.2T]$s. The reconstruction error was evaluated in the region of $[-1, 1]$ to mitigate the end effects. To evaluate the reconstruction performance, we compute the log-error energy between the $x(t)$ and the k^{th} output $x_k(t)$. Although the result shows that warped sinc interpolation achieves a better convergence than linear interpolation, the error of both methods did not converge to zero. This might be due to finite precision error obtained in the simulation. Future work can be done to improve the convergence properties of the iterative algorithm in the simulation.

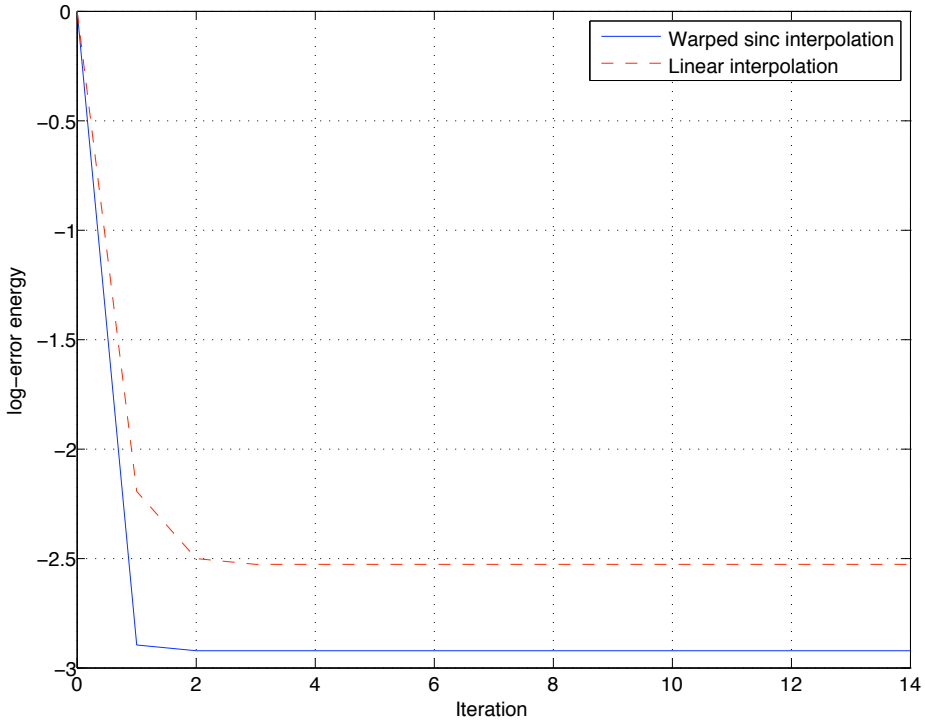

Figure 5-5: Illustration of iterative reconstruction algorithm.

Bibliography

[1] R. Amirtharajah, J. Collier, J. Siebert, B. Zhou and A. Chandrakasan, "DSPs for energy harvesting sensors: applications and architectures", *IEEE Pervasive Computing*, vol. 4, no. 3, pp. 72-79, July 2005.

[2] A. Aldroubi, M. Unser and M. Eden, "Cardinal spline filters: stability and convergence to the ideal sinc interpolator", *Signal Process.*, vol. 28, no. 2, pp. 127-138, August 1992.

[3] R. T. Behrens and L. L. Scharf, "Signal processing applications of oblique projection operators," *IEEE Trans. Signal Processing*, vol. 42, no. 6, June 1994.

[4] M. A. Blanco and F. S. Hill, Jr, "On time warping and the random delay channel," *IEEE Trans. Information Theory*, vol. IT-25, no. 2, March 1979.

[5] J. J. Clark, M. R. Palmer and P. D. Lawrence, "A transformation method for the reconstruction of functions from nonuniformly spaced samples," *IEEE Trans. Acoust., Speech, Signal Processing*, vol. ASSP-33, no. 4, pp. 1151-1165, October 1985.

[6] C. D. Boor, "On calculating with b-splines," *J. Approximat. Theory*, vol. 6, pp. 50–62, 1970.

[7] Y. C. Eldar, "Sampling with arbitrary sampling and reconstruction spaced and oblique dual frame vectors," *J. Fourier Anal. Appl., vol. 1, no. 9, pp. 77-96, January 2003.*

[8] Y. C. Eldar and A. V. Oppenheim, "Filterbank reconstruction of bandlimited signals from nonuniform and generalized samples," *IEEE Trans. Signal Processing*, vol. 48, no. 10, pp. 2864-2875, October 2000.

[9] H. G. Feichtinger and K. Gröchenig, "Irregular sampling theorems and series expansions of band-limited functions," *J. Math. Anal. and Appl.*, vol. 167, pp. 530-556, 1992.

[10] H. G. Feichtinger, K. Gröchenig and T. Strohmer, "Efficient numerical methods in non-uniform sampling theory," *Numerische Mathematik*, vol. 69, no. 4, pp. 423-440, July 1995.

[11] K. Gröchenig, "Reconstruction algorithms in irregular sampling," *Math. Comp.*, vol. 59, no. 199, pp. 181-194, July 1992.

[12] B. Gold, A. V. Oppenheim and C. M. Rader, "Theory and implementation of the discrete Hilbert transform," *Symposium on Computer Processing in Communications (Polytechnic Institute of Brooklyn)*, April 8-10, 1969.

[13] J. R. Higgins, *Sampling Theory in Fourier and Signal Analysis: Foundations*, Oxford Science Publications, Clarendon Press, Oxford, 1996.

[14] J. R. Higgins, "A sampling theorem for irregularly spaced sample points," *IEEE Trans. Information Theory*, vol. 22, no. 5, pp. 621-622, September 1976.

[15] M. I. kadec, "The exact value of the Paley-Wiener constant," *Soviet Math. Dokl.*, vol. 5, pp. 559-561, 1964.

[16] H. J. Landau, "Necessary density conditions for sampling and interpolation of certain entire functions," *Acta Mathematica*, vol. 117, no. 1, pp. 37-52, July 1967.

[17] H. J. Landau, "Sampling, Data Transmission, and the Nyquist rate," *Proc. IEEE*, vol. 55, no. 10, pp. 1701-1706, October 1967.

[18] N. Levinson, *Gap and Density Theorems*, New York: A.M.S., 1940.

[19] F. Marvasti, *Nonuniform Sampling*, New York: Kluwer Academic, 2001.

[20] F. Marvasti, M. Analoui and M. Gamshadzahi, "Recovery of signals from nonuniform samples using iterative methods," *IEEE Trans. Signal Processing*, vol. 39, no. 4, April 1991.

[21] R. A. C. Paley and N. Wiener, *Fourier Transforms in the Complex Domain*, New York: A.M.S., 1934.

[22] A. Papoulis, "Error analysis in sampling theory," *Proc. IEEE*, vol. 54, no. 7, pp. 947-955, July 1966.

[23] A. Russell, "Regular and Irregular Signal Resampling," Ph.D. thesis, Massachusetts Institute of Technology, Cambridge, MA, June 2002.

[24] L. L. Schumaker, *Spline Functions: Basic Theory*, New York: Wiley, 1981.

[25] S. S. Senturia and B. D. Wedlock, *Electronic Circuits and Applications*, John Wiley, 1975.

[26] S. Dey. Private Communication.

[27] S. Tertinek and C. Vogel, "Reconstruction of nonuniformly sampled bandlimited signals using a differentiator-multiplier cascade," *IEEE Trans. Circuits and Systems*, vol. 55, no. 8, pp. 2273-2286, September 2008.

[28] M. Unser, A. Aldroubi, and M. Eden, "On the asymptotic convergence of B-spline wavelets to Gabor functions," *IEEE Trans. Information Theory,* vol. 38, no. 2, pp. 864-872, 1992.

[29] D. Wei, "Sampling based on local bandwidth," *Proceedings of the 41st Annual Asilomar Conference on Signals, Systems, and Computers (Asilomar, CA),* November 4-7 2007.

[30] R. G. Wiley, "Recovery of band-limited signals from unequally spaced samples," *IEEE Trans. Commun.*, vol. COM-26, no. 1, January 1978.

[31] J. Xu and L. Zikatanov, "The method of alternating projections and the method of subspace corrections in Hilbert space," *J. American Mathematical Society*, vol. 15, no. 3, pp. 573-597, April 2002.

[32] K. Yao and J. B. Thomas, "On some stability and interpolatory properties of nonuniform sampling expansions," *IEEE Trans. Circuit Theory*, vol. 14, no. 4, pp. 404-408, December 1967.

[33] J. L. Yen, "On nonuniform sampling of bandwidth-limited signals," *IRE Trans. Circuit Theory*, vol. 3, no. 4, pp. 251-257, December 1956.

[34] R. M. Young, *An Introduction to Nonharmonic Fourier Series - revised first edition*, San Diego: Academic Press, 2001.

[35] L. A. Zadeh, "Correlation functions and spectra of phase- and delay-modulated signals," *Proc. I.R.E.*, vol. 39, no. 4, pp.425-428, April 1951.

[36] Y. Y. Zeevi and E. Shlomot, "Nonuniform Sampling and Antialiasing in Image Representation," *IEEE Trans. Signal Processing*, vol. 41, no. 3, pp. 1223-1236, March 1993.